Memoirs of the Faculty of Engineering, Nagoya University
Vol. 32, No. 2 (1980)

TSC AND TL STUDIES OF CARRIER TRAPPING IN INSULATING POLYMERS

MASAYUKI IEDA, TERUYOSHI MIZUTANI and YASUO SUZUOKI

Department of Electrical Engineering

(Received October 27, 1980)

Abstract

The techniques of the X-ray induced thermally stimulated current (TSC) and thermoluminescence (TL) are pointed out to be powerful to investigate the natures and the origins of carrier traps in insulating materials and they are systematically applied to various polymers, especially to polyethylene.

Most polymers except those of high ionic conduction such as polyvinyl chloride, show remarkable TSC peaks arising from trapped carriers and some of them are accompanied with TL peaks. Most of TSC (TL) peaks correspond well to the onset of molecular motions, suggesting that the molecular motions strongly affect the release of electrons (holes) from traps. In highly crystalline polymers such as polyethylene and polytetrafluoroethylene, several TSC peaks appear above the glass transition temperatures and originate from traps in the crystalline regions and / or in their boundary regions.

Some of carrier traps are ascribed to physical defects such as cavities formed by local arrangements of polymer chains. In this case, the erosion of traps by molecular motions may promote the detrapping of electrons (holes). The locations of these traps are also determined from the corresponding molecular motions which have already been understood well.

In polyethylene, for example, five or six kinds of traps are assigned to physical defects such as cavities. Oxidation products such as the carbonyl groups and the cross-linking points also act as fairly deep traps.

CONTENTS

1. Introduction

Synthetic polymeric materials have been used extensively as electrical insulators because of their high electric strength and good dielectric and mechanical properties. The world-wide tendency to use ultra-high voltage and DC transmission systems makes the demand for better polymer insulators increasingly greater and especially urgent. Many factors are known to affect the electrical breakdown of polymers. Among them, the space charge effect is one of the most important and serious problems.[1~3]

Insulating polymers also show an extremely good charge-storage capability and have received wide applications such as electrets[4] and xerographic photoreceptors.[5] In recent years, polymer electrets have been utilized not only as electret transducers (microphones, earphones, etc.), but also as gas filters, motors, relay switches, optical display systems and radiation dosimetry. Moreover, the discovery of the strong piezoelectric and pyroelectric properties of some polymer electrets around 1970 promoted new electret applications such as electromechanical transducers (including electroacoustic transducers) and light detectors (including vidicons).[6]

Both space charge and charge-storage capability are closely related to carrier traps. The details about carrier traps in polymers, however, are not yet understood. To improve polymeric insulators and to develop such practical applications mentioned above, it is necessary to clarify the natures and the origins of carrier traps.

The recent application of thermally stimulated current (TSC) and thermoluminescence (TL) techniques has produced a great deal of information about carrier traps in polymeric insulators.[4, 7~10] This paper concerns the study of carrier traps in various polymers, especially in polyethylene, by the X-ray induced TSC and TL techniques.

2. Theories of X-ray Induced TSC and TL

2. 1. X-ray Induced TSC and TL

The mechanisms of X-ray induced TSC and TL are illustrated in Fig. 1. The X-ray irradiation produces free electrons (holes) in an insulator and some of them are captured by electron (hole) traps at a low temperature, T_1. When the specimen is heated linearly under the application of a DC field, the thermal release of electrons (holes) from their traps results in TSC. Some of released electrons recombine radiatively with holes in recombination centers, thus giving rise to TL (Fig.

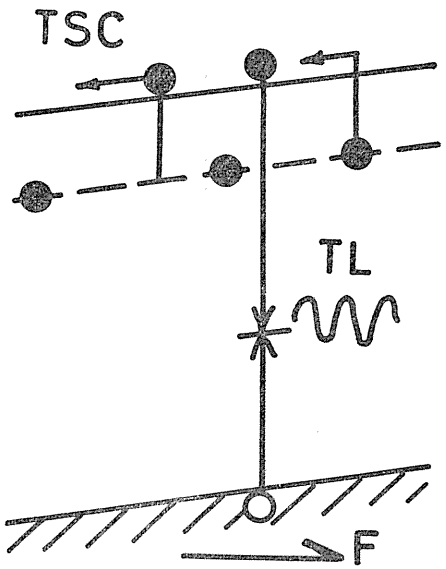

Fig. 1. TSC and TL from trapped electrons.

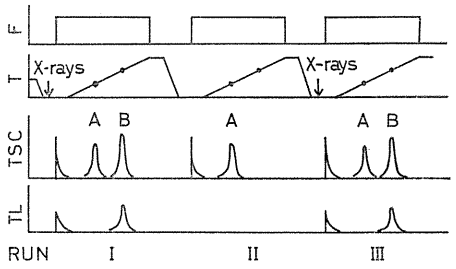

Fig. 2. X-ray induced TSC and TL. Peak A and B are from dipoles and trapped carriers, respectively.

1).

The X-ray induced TSC and TL techniques are helpful to distinguish between a TSC peak by dipole orientation and that originating from carrier detrapping.[11~12] Figure 2 shows a series of TSC experiments. The previous X-ray excitation results in both dipole (A) and carrier (B) peaks in runs I and III, while without previous X-ray excitation only a dipole peak (A) is observed in run II. Moreover, a TL peak is accompanied with the carrier peak (B), but not with the dipole peak (A). Thus, the comparison of the TSC (TL) spectra with and without the previous X-ray excitation enables us to distinguish between dipole and carrier peaks.

2. 2. TSC from Trapped Carriers

For simplicity, we will deal with the band conduction and a single set of electron traps with energy E_t and density N_t. The following equations express the rates at which the densities of conduction and trapped electrons change after the filling of traps by some excitation in the monomolecular recombination case:

$$\frac{dn_t}{dt} = -n_t \nu \exp\left(-\frac{E_t}{kT}\right) + n_c(N_t - n_t)S_t v, \tag{1}$$

$$\frac{dn_c}{dt} = -\frac{dn_t}{dt} - \frac{n_c}{\tau}, \tag{2}$$

where n_c, v, τ are the density, the thermal velocity and the recombination lifetime of the conduction-band electrons, S_t is the capture cross section of the traps, ν ($=N_c S_t v$, N_c: the density of the states in the conduction band) the attempt-to-escape frequency of trapped electrons, T the absolute temperature and k the Boltz-

mann constant (Fig. 3).

By using n_c obtained from these two equations, the theoretical expression for the thermally stimulated current (TSC) density $J(T)$ under a uniform external field is given by

$$J(T)=qn_c\mu F, \tag{3}$$

where q, μ are the charge and the mobility of electron respectively, and F is the applied field.

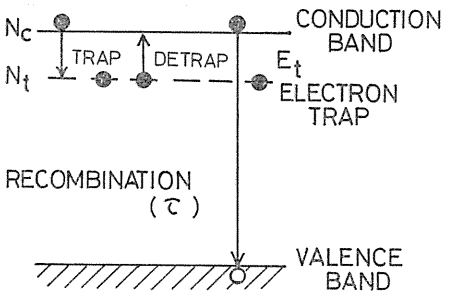

Fig. 3. Simplified band model with a single set of electron traps.

The expressions for TSC have been obtained in the following cases.[13]

(I) Fast retrapping case $[(N_t-n_t)S_tv\gg\tau^{-1}]$

In the case that the retrapping of detrapped electrons dominates the recombination, the density ratio of conduction band electrons to trapped ones can be given by

$$\frac{n_c}{n_t}=\frac{N_c}{N_t}\exp\left(-\frac{E_t}{kT}\right). \tag{4}$$

Let

$$n=n_c+n_t. \tag{5}$$

From Eqs. (4) and (5), we have

$$n=n_c\left[1+\frac{N_t}{N_c}\exp\left(\frac{E_t}{kT}\right)\right]\simeq n_c\frac{N_t}{N_c}\exp\left(\frac{E_t}{kT}\right). \tag{6}$$

Equations (2) and (5) give

$$\frac{dn}{dt}=-\frac{n_c}{\tau}. \tag{7}$$

Substituting Eq. (6) into Eq. (7) gives

$$\frac{d}{dt}\left[n_c\cdot\frac{N_t}{N_c}\exp\left(\frac{E_t}{kT}\right)\right]=-\frac{n_c}{\tau}. \tag{8}$$

Solving Eq. (8) for a uniform rise rate of temperature ($T=T_1+\beta t$), we get

$$n_c=n_{c0}\exp\left(\frac{E_t}{kT_1}\right)\exp\left[-\frac{E_t}{kT}-\frac{N_c}{\beta\tau N_t}\int_{T_1}^{T}\exp\left(-\frac{E_t}{kT'}\right)dT'\right] \tag{9}$$

where n_{c0} is the density of conduction-band electrons at $T=T_1$. Let n_{t0} be the density of the occupied traps at $T=T_1$, then Eq. (4) gives

$$n_{c0}=n_{t0}\frac{N_c}{N_t}\exp\left(-\frac{E_t}{kT_1}\right). \tag{10}$$

From Eqs. (9) and (10), we have

$$n_c=\frac{n_{t0}N_c}{N_t}\exp\left[-\frac{E_t}{kT}-\frac{N_c}{\beta\tau N_t}\int_{T_1}^{T}\exp\left(-\frac{E_t}{kT'}\right)dT'\right]. \tag{11}$$

Therefore, TSC is given by

$$J(T)=\frac{q\mu n_{t0}FN_c}{N_t}\exp\left[-\frac{E_t}{kT}-\frac{N_c}{\beta\tau N_t}\int_{T_1}^{T}\exp\left(-\frac{E_t}{kT'}\right)dT'\right]. \tag{12}$$

(Ⅱ) Slow retrapping case $[(N_t-n_t)\ S_t v\ll\tau^{-1}]$

In this case, Eqs. (1) and (2) are approximated by

$$\frac{dn_t}{dt}=-n_t\nu\exp\left(-\frac{E_t}{kT}\right), \tag{13}$$

$$0=-\frac{n_c}{\tau}-\frac{dn_t}{dt}, \tag{14}$$

as it is assumed that $dn_c/dt\ll dn_t/dt$.

Solving Eq. (13), we get

$$n_t=n_{t0}\exp\left[-\frac{\nu}{\beta}\int_{T_1}^{T}\exp\left(-\frac{E_t}{kT'}\right)dT'\right]. \tag{15}$$

Substituting Eq. (15) into Eq. (14) gives

$$n_c=n_{t0}\tau\nu\exp\left[-\frac{E_t}{kT}-\frac{\nu}{\beta}\int_{T_1}^{T}\exp\left(\frac{E_t}{kT'}\right)dT'\right]. \tag{16}$$

Then TSC is given by

$$J(T)=q\mu n_{t0}\tau\nu F\exp\left[-\frac{E_t}{kT}-\frac{\nu}{\beta}\int_{T_1}^{T}\exp\left(-\frac{E_t}{kT'}\right)dT'\right]. \tag{17}$$

(Ⅲ) High field case

In case the applied field is so high that detrapped electrons are swept out into the electrode without retrapping or recombination, TSC can be expressed by

$$J(T)=\int_0^a q\left(-\frac{dn_t}{dt}\right)\frac{x}{d}dx \tag{18}$$

where d is the thickness of a specimen. As the rate of the change in n_t is expressed by Eq. (13), n_t is given by Eq. (15). Substituting this into Eq. (18), we have

$$J(T)=\frac{qdn_{t0}\nu}{2}\exp\left[-\frac{E_t}{kT}-\frac{\nu}{\beta}\int_{T_1}^{T}\exp\left(-\frac{E_t}{kT'}\right)dT'\right]. \tag{19}$$

In the cases (Ⅰ), (Ⅱ) and (Ⅲ), TSC can be expressed by

$$J(T)=A\exp\left[-\frac{E_t}{kT}-\frac{B}{\beta}\int_{T_1}^{T}\exp\left(-\frac{E_t}{kT'}\right)dT'\right] \tag{20}$$

where A and B are constants (Table 1). The TSC shows a peak at $T=T_m$ (Fig. 4),

Table 1. Values of A and B in Eq. (20).

	Fast Retrapping	Slow Retrapping	High Field
A	$\frac{qn_{to}N_cF}{N_t}$	$q\mu n_{to}\tau\nu F$	$\frac{qdn_{to}\nu}{2}$
B	$\frac{N_c}{\tau N_t}$	ν	ν

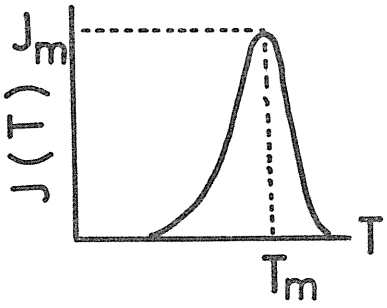

Fig. 4. Typical TSC curve from trapped electrons.

$$\frac{\beta}{B}=\frac{kT_m^2}{E_t\exp\left(\frac{E_t}{kT_m}\right)} \tag{21}$$

The low temperature tail of Eq. (20) is approximated by

$$J(T)=A\exp\left(-\frac{E_t}{kT}\right). \tag{22}$$

The trap depth E_t can be determined from the slope of the low temperature tail of $J(T)$ plotted in $\ln J(T)$ versus $1/T$ (the initial rise method).[14]

2. 3. TSC from Dipoles[12]

In general, the build-up of polarization can be described by

$$\frac{dP(t)}{dt}=-\frac{P-P_0}{\tau_d}, \tag{23}$$

$$P_0=\frac{N_d\mu_d^2F}{3kT}, \tag{24}$$

where τ_d is relaxation time of dipole, N_d is the concentration of dipoles, μ_d is the dipole moment, and F is the applied bias field. The temperature variation of τ_d may be represented by $\tau_d=\tau_0\exp(H/kT)$ where τ_0^{-1} is the characteristic frequency factor and H is the activation energy.

Assuming $P(t)=0$ at $t=0$, we get

$$P(t)=P_0\{1-\exp[-\int_0^t\tau_0^{-1}\exp(-H/kT)dt]\}. \tag{25}$$

Considering that $T=T_1+\beta t$, the thermally stimulated polarization current $J_d(T)$ $(=\mathrm{d}P(t)/\mathrm{d}t)$ is written

$$J_d(T)=\frac{P_0}{\tau_0}\exp\left[-\frac{H}{kT}-\frac{1}{\beta\tau_0}\int_{T_1}^{T}\exp\left(-\frac{H}{kT}\right)\mathrm{d}T\right]$$

$$=\frac{N_d\mu_d^2F}{\tau_0 3kT}\exp\left[-\frac{H}{kT}-\frac{1}{\beta\tau_0}\int_{T_1}^{T}\exp\left(-\frac{H}{kT}\right)\mathrm{d}T\right]. \tag{26}$$

Then, the activation energy H can be estimated from the slope of the low-temperature $J_d(T)$ tail plotted in the $\ln J_d(T)$-vs-$1/T$ plot. The condition for the maximum of Eq. (26), neglecting the temperature dependence of P_0, yields

$$\beta\tau_0=kT_m^2[H\exp(H/kT_m)]^{-1}. \tag{27}$$

Since the polarization $P(T)$ can be approximated by $P_0(T)$ in the high-temperature region, the current is expressed by

$$J_d(T)=\beta\frac{\mathrm{d}P(T)}{\mathrm{d}T}=\beta\frac{\mathrm{d}P_0(T)}{\mathrm{d}T}=-\frac{\beta N_d\mu_d^2F}{3kT^2}. \tag{28}$$

From Eqs. (27) and (28), the current $J_d(T)$ shows a current peak and then a current inversion with increasing temperature (Fig. 5).

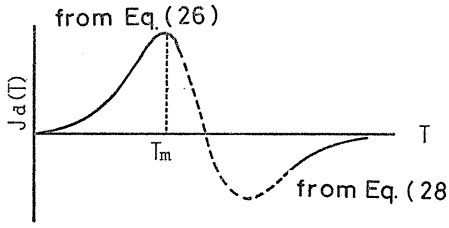

Fig. 5. Typical TSC curve from dipoles.

2. 4. X-ray Induced TL

The intensity I of thermoluminescence (TL) is given by

$$I=-\eta\frac{\mathrm{d}n_t}{\mathrm{d}t} \tag{29}$$

where η is a constant of proportionality. Therefore, the theoretical expression for TL can be obtained by using the equations derived in the case of TSC (§ 2. 1).

$$I=A'\exp\left[-\frac{E_t}{kT}-\frac{B}{\beta}\int_{T_1}^{T}\exp\left(-\frac{E_t}{kT'}\right)\mathrm{d}T'\right]. \tag{30}$$

The evaluation of E_t and other parameters can also be made in the similar way to TSC.

3. Experimental Details

3. 1. Specimens

Specimens used are polymer films, which are summarized in Table 2. Thin Au electrodes (30mmϕ) were evaporated on both sides of a specimen at 2×10^{-5} Torr. The details of the specimens will be given later in each chapter.

3. 2. Experimental Apparatus

Figure 6 shows a schematic diagram of the experimental set-up for measuring X-ray induced TSC and TL. The temperature of the electrode system in a vacuum vessel is controlled from 90 to 540K by an electric heater and liquid nitrogen. X-rays were generated by an X-ray tube (Toshiba AFX-61AW, W target) under the conditions of 40kV and 30 mA, and were irradiated to the specimen at a distance of 12 cm through a 50-μm-thick Al window. The TSC was measured with a vibrating reed electrometer (Takeda, TR-84M) and the TL was observed with a photomultiplier tube (R-106UH, HTV).

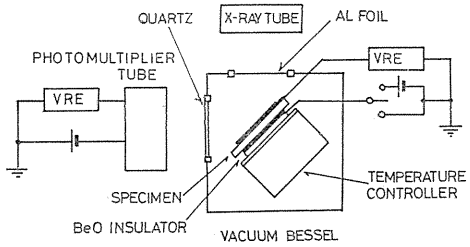

Fig. 6. Block diagram for measuring X-ray induced TSC and TL.

In the experiment of PSDC, exciting monochromatic light was obtained by using a 500 W xenon lamp (Ushio Electric Inc.) and a monochromator (Shimazu Baush & Lomb). Spurious light was removed by a suitable colored-glass filter placed between the monochromator and the quartz window of the vacuum vessel.

3. 3. Experimental Procedures

3. 3. 1. X-ray induced TSC

The experimental procedure of the X-ray induced TSC is illustrated in Fig. 7. First, a specimen set on the electrode system was cooled to a low temperature T_1 (90K) in vacuum (0.1Pa) and irradiated with X-rays for 20 minutes under a short-circuit condition in order to fill traps with electrons (holes). The bias voltage was then applied and the current through the specimen was monitored. After the transient current was reduced to a negligibly small value, the specimen was heated up at a rate of 6 K/min from T_1 to a high temperature T_2 near the melting point of the specimen. A TSC spectrum was recorded with a recorder connected to a vibrating reed electrometer. Hereafter, this is referred to as TSC with X-ray irradiation.

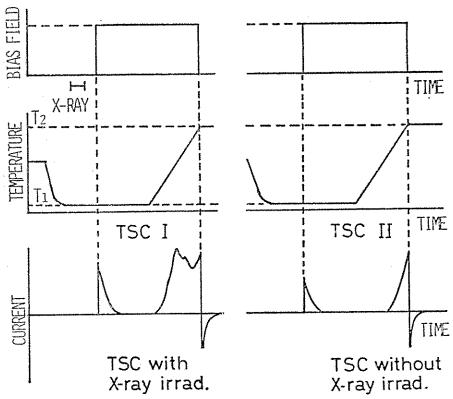

Fig. 7. Procedure for TSC measurement.

Table 2. List of specimens used.

Specimen	Code	Formula (H is abbreviated.)	T_m(K)	X_c(%)	d(μm)
Polyethylene HD-PE MD-PE LD-PE	PE	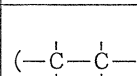	381 399 408	43-47 55-60 82-85	25-30 25 25-30
Ethylene-Vinyl Acetate Copolymer	EVA	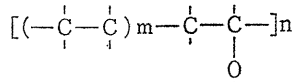	358-370	19-35	30
Polypropylene	PP	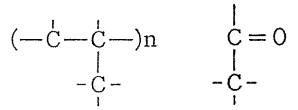	440	high	20-25
Polyvinyl Chloride	PVC	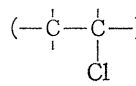			20-30
Polyvinyl Fluoride	PVF	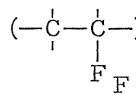	463-473		55
Polyvinylidene Fluoride	PVDF	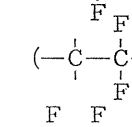	438-458	50	15-50
Polytetrafluoro-ethylene	PTFE	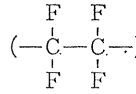	600	70	55
Ethylene-Tetrafluoroethylene Copolymer.	ETFE	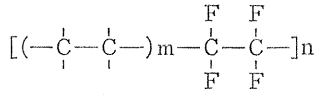	543	50	25
Tetrafluoroethylene-Hexafluoropropylene Copolymer	FEP	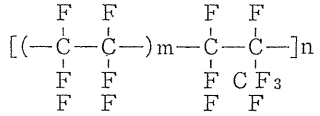	560	35	25
Tetrafluoroethylene-Perfluoroalkilether Copolymer	PFA	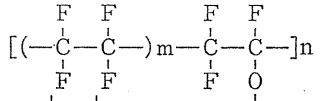	575-579		25
Polystyrene	PS	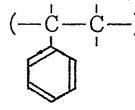		0	30
Poly-p-Xylylene	PPX	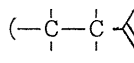	672	37-51	6-10
Polyethylene Terephthalate	PET	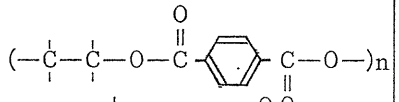	533	41	25
Polycarbonate	PC	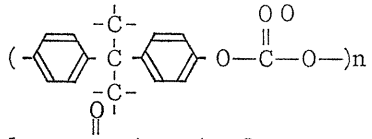		0	30
Nylon·6		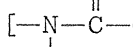	496		21

T_m the melting temperature, X_c the crystallinity, d the thickness

The TSC without preceding X-ray irradiation was also observed under the same condition except no X-ray irradiation. In this case, as there has been no X-ray irradiation and, thus, no trapped carriers, the TSC spectrum has no contribution of trapped carriers. Therefore, the difference between these two TSC spectra may be due to the thermal release of trapped carriers.

3. 3. 2. X-ray induced TL

Figure 8 shows the experimental procedure for measuring X-ray induced TL. A specimen was cooled to 90 K in vacuum (0. 1 Pa) and then irradiated with X-rays for 20 minutes. After the isothermal luminescence was measured at 90 K for 90 minutes, TL was measured at a heating rate of 6 K/min with a photomultiplier tube.

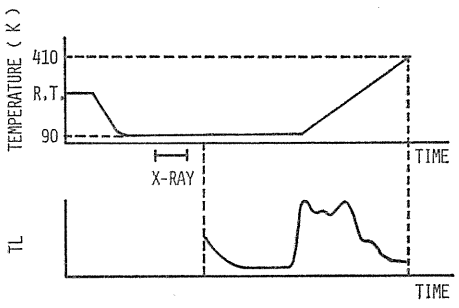

Fig. 8. Procedure for TL measurement.

3. 3. 3. Photo-stimulated detrapping current (PSDC)

In the PSDC experiment, semi-transparent Au electrodes were evaporated onto the specimen so that the exciting light could go through them. The specimen set in the vacuum vessel was cooled to 90 K in vacuum (0. 1 Pa) and irradiated with X-rays under the same condition as in § 3. 3. 1. Then the bias voltage of 90 V was applied to the specimen and photocurrents excited by monochromatic light were observed after the transient dark current decreased to a small value. Photocurrent measurements were repeated at 90 K after the thermal elimination of some of the TSC peaks by heating up the specimen.

4. X-ray Induced TSC in Polyethylene

4. 1. Introduction

Because of its high-resistivity and low-tanδ characteristics, polyethylene has been used widely as insulating materials for power cables and communication cables. Also because it has the simplest chemical structure among polymers, polyethylene has been studied extensively by many researchers. Many reports have been published on TSC and TL in polyethylene.[12, 15~19] Carbonyl groups introduced by oxidation,[20, 21] physical defects such as microcavities[12, 19] and free radicals[22] have been proposed to act as carrier traps.

Recently much attention has been paid to understanding the electrical properties of polymers in molecular or morphological terms. For this purpose, polyethylene is a good prototype. Polyethylene (PE) has three morphologically-different forms, i. e. HD-PE (high-density PE) MD-PE (medium-density PE) and LD-PE (low-density PE). HD-PE is produced at low pressure by Ziegler-Natta catalists and it has the least branching, the highest density (0. 95-0. 97 g/cm^3) and the highest crystallinity (>70%). LD-PE is polymerized by a free radical mechanism with peroxide initiators under high pressure and it has the lowest density (0. 91-0. 93 g/

cm^3) and the lowest crystallinity (40–50%). Moreover, ethylene can be easily copolymerized with vinyl acetate (VA) by the high pressure process to yield a range of copolymers having a wide variety of physical properties. The incorporation of VA units into a polyethylene backbone chain reduces the crystallinity of PE.

Therefore, PE and ethylene-vinyl acetate copolymer (EVA) are suitable to examine the relation between carrier traps and the morphology of PE. Since the VA monomer unit includes in its chemical structure a carbonyl group, the TSC in EVA may offer some information about the relation between carrier traps and carbonyl groups.

In this chapter, the X-ray induced TSC spectra in PE and EVA have been investigated. The natures and the origins of carrier traps have been discussed.

4. 2. Experimental

Specimens used in this chapter were films of HD-PE, MD-PE, LD-PE, EVA and XL-PE (cross-linked PE : gel fraction ~70%). They were supplied from the Mitsubishi Petrochemical Corp. and were nominally free from antioxidants and other additives. EVA's containing 6.0, 12.5, 16.5 and 22.0 wt. % of VA are referred to as EVA-1, EVA-2, EVA-3 and EVA-4, respectively. The physical properties of the specimens are summarized in Table 3.

Table 3. Physical properties of specimens used.

specimen	melt index	density (g/cm^3)	vinyl acetate content (wt%)
HD-PE	2.6	0.960	
MD-PE	1.0	0.932	
LD-PE	4.0	0.918	0
EVA-1	6.0	0.923	6.0
EVA-2	3.3	0.933	12.5
EVA-3	1.8	0.938	16.5
EVA-4	9.2	0.943	22.0
XL-PE	—	0.919	

To examine the oxidation effects, some of PE specimens were oxidized at room temperature by exposure to an ozone atmosphere produced by the gas discharge in oxygen. The extent of oxidation was estimated from the infrared absorption of the main carbonyl stretching at about 1720 cm^{-1}. Oxidized specimens are summarized in Table 4.

Some of them were irradiated with γ-rays from ^{60}Co at room temperature in an ampoule evacuated to 0.1 Pa. Under these irradiation conditions, PE films were hardly oxidized (infrared absorption coefficient of the irradiated PE at about 1720 $cm^{-1} \simeq 0$).

Table 4. List of specimens.

specimen		oxidizing time	absorption coefficient at about 1720cm^{-1}
HD-PE	A	0 min	—
	B	35	1.1 cm^{-1}
	C	400	17
	D	450	40
	E	400	68
LD-PE	A	0	—
	B	400	21
	C	400	72
	D	720	172

4. 3. Results and Discussions

4. 3. 1. TSC spectra of PE and EVA

Figure 9 shows typical TSC spectra with and without X-ray irradiation for LD-PE, together with the TL spectrum and the mechanical loss curve (Δ_G). Their peak temperatures correspond well each other. The TSC spectrum I with previous X-ray irradiation shows five TSC peaks designated by C_1, C_2, C_3, C_4 and C_5 in ascending order of temperature. On the other hand, the TSC II without X-ray irradiation is too small to detect any TSC peak except the steady-state conduction current above 320 K. The five TSC peaks in the TSC I must be due to trapped carriers introduced by prior irradiation, since the TSC II, that of non-irradiated specimen, shows no TSC peaks. Any TSC peak from dipoles was not observed because LD-PE contained hardly any dipoles.

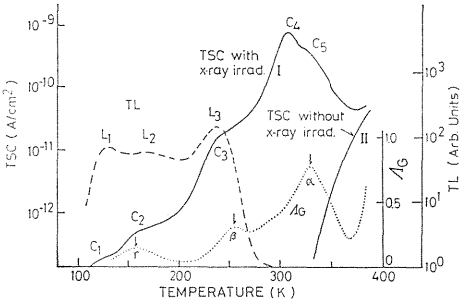

Fig. 9. TSC spectra for LD-PE under a field of 90 kV/cm, together with the TL spectrum and the mechanical loss curve (Δ_G).[30]

The X-ray irradiated HD-PE exhibits six TSC peaks designated C_1–C_5 and C_5' (Fig. 10). Figure 11 shows the morphology-dependence of the TSC spectra. The C_4 and C_5 (C_5') peaks in the high temperature region strongly depend upon the degree of crystallinity.

Figure 12 and 13 show typical TSC spectra for EVA-1 and EVA-4, respectively. The TSC spectrum I for EVA-1 exhibits five TSC peaks corresponding to C_1–C_5 peaks of LD-PE and an additional C_3' peak. In EVA-4, the C_3' peak is hidden under the larger C_4 peak (Fig. 13). The TSC spectrum II for EVA shows a prominent peak (C_6) and a current inversion. Since the vinyl acetate unit of EVA has the permanent dipole moment of 1.7 D,[22] the current inversion following the C_6 peak is concluded to be due to dipoles as theoretically expected in § 2. 3.

In Figs. 14 and 15, the apparent trap depth E_t for LD-PE and HD-PE evalu-

ated from the partial heating[24] is plotted against the maximum temperature in each partial heating.

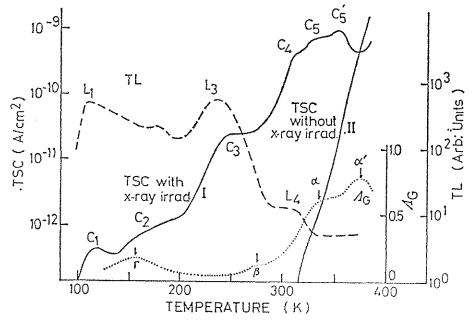

Fig. 10. TSC spectra for HD-PE under a field of 90 kV/cm, together with the TL spectrum and the mechanical loss curve (Δ_G).[30]

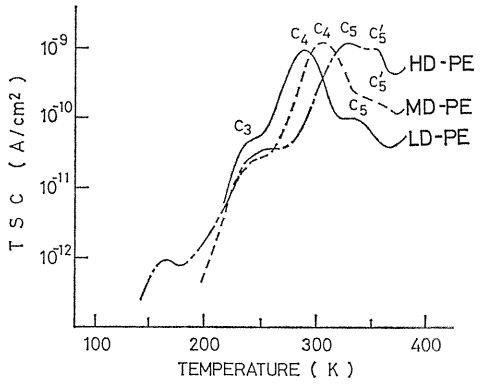

Fig. 11. X-ray induced TSC spectra for LD-PE, MD-PE and HD-PE. (field: 90 kV/cm)

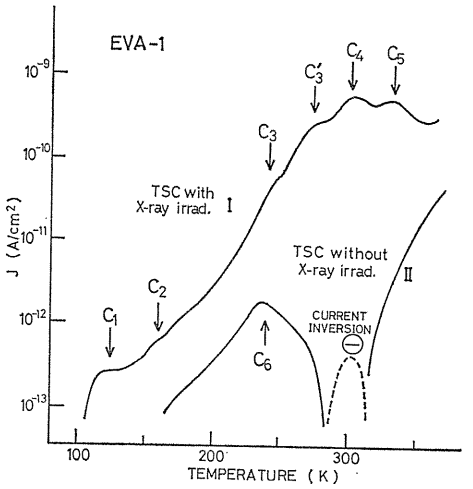

Fig. 12. TSC spectra for EVA-1 under a field of 90 kV/cm.

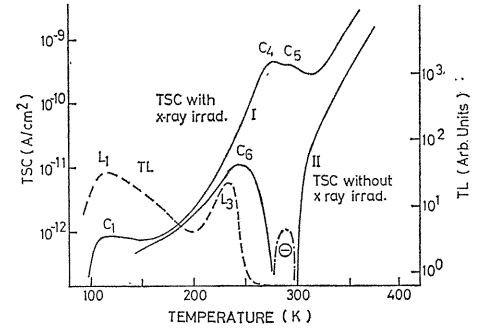

Fig. 13. TSC spectra for EVA-4 under a field of 90 kV/cm, together with the TL spectrum.

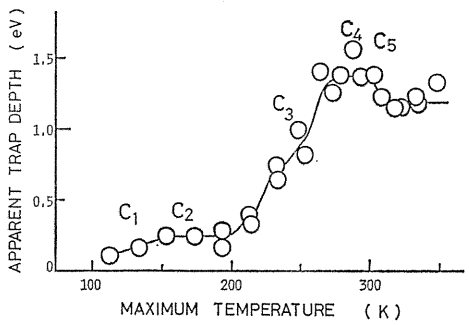

Fig. 14. Apparent trap depth E_t versus the maximum temperature reached in each partial heating for LD-PE irradiated with X-rays.

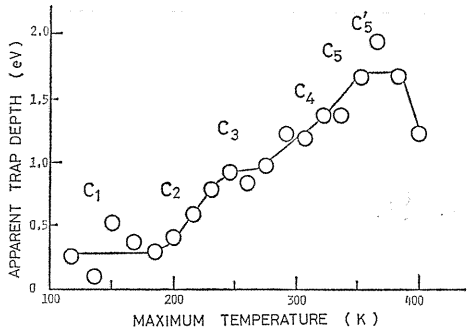

Fig. 15. Apparent trap depth E_t versus the maximum temperature reached in each partial heating for HD-PE irradiated with X-rays.

4. 3. 2. Origins of TSC peaks

Fowler[25] observed the increased dark conductivity in polyethylene after X-ray irradiation which decayed with an extremely long time constant at room temperature and he explained it by the release of trapped carriers into the conduction (or valence) band. The remarkable enhancement of TSC by prior irradiation is closely related to the residual dark conductivity. Also, the existence of the broad bands in polyethylene has been proved by the theoretical band calculation[26] and ESCA experiment.[27] Some of free electrons (holes) excited by X-ray irradiation are captured by traps at 90 K. Therefore, it seems reasonable to explain the TSC peaks C_1–C_5 by the release of trapped carriers into the conduction (or valence) band. TSC peaks C_1–C_3 are accompanied with strong TL peakes (Figs. 9 and 10), which supports the above model.

In Fig. 16, the peak temperature of the observed TSCs are plotted against the vinyl acetate content and the resulting curves are compared with those of the relaxation tests at about 1 c/s,[28] because the TSC experiments are considered to reflect the relaxation at very low frequencies.[29] α and β represent loss peaks due to the corresponding relaxations. The α relaxation is assigned to the crystalline region and its peak temperature decreases with increasing vinyl acetate content. The β relaxation is related to segmental motions in the amorphous region.[28] As shown in Fig. 16, the peak temperatures of C_3 and C_5 almost coincide with those of the α and β loss peaks, respectively. In highly crystalline HD-PE, the α loss peak has been reported to split into two components, α and α'.[30] The C_5 peak of

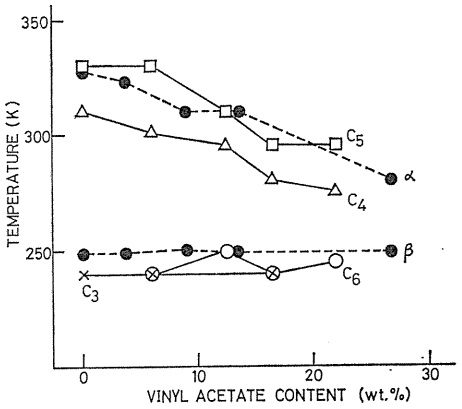

Fig. 16. TSC peak temperature versus vinyl-acetate content, together with the peak temperatures of the mechanical losses.[28]

HD-PE has also split into C_5 and C_5' which appear near the peak temperatures of the α and α' loss peaks (Fig. 10). The C_2 peak also appears around the temperature where the γ loss peak occurs[31] (Figs. 9 and 10). These suggest the close correlation between the release of trapped carriers and molecular motions.[18, 32, 33] The above discussions lead to the following assignment of traps corresponding to the TSC peaks:

C_2: traps whose detrapping is enhanced by the γ relaxation.

C_3: traps in the amorphous region whose detrapping is enhanced by the β relaxation.

C_5: traps in the crystalline region whose detraping is enhanced by the α relaxation.

The assignment of the traps corresponding to the C_4 peaks is not clear but they may be associated with the boundary region between the crystalline and amorphous regions for the following reasons:

(i) Some trapping sites have been reported to be located in the amorphous-crystalline boundaries of polyethylene.[34, 35]

(ii) The C_4 peak appears in the temperature range between the α and β relaxations.

Now we shall discuss the origin of traps. Trapping sites in polyethylene have been reported to be ascribed to carbonyl groups produced by oxidation[20,21] or to physical defects such as cavities formed by local arrangements of molecular chains.[12, 19] A TSC peak ascribed to electrons trapped in carbonyl groups would be expected to be enhanced with increasing vinyl acetate content. Actually, there is no remarkable difference in magnitude among TSCs in LD-PE and EVA and it does not offer any strong evidence for the assumption that the carbonyl groups are trapping sites, except for the C_3' peak. Moreover the C_3' peak cannot be easily resolved except in EVA-1. Therefore, the assignment of the C_3' peak to the carbonyl group must be reserved for future work. The TSC spectra of PE and EVA above room temperature strongly depend upon its crystallinity or its morphology as shown in Fig. 11 and 16. Ekstrom and Willard have reported that many properties of electron traps in various organic glasses can be explained by cavity traps.[31] The existence of cavity traps formed by local arrangements of molecular chains seems very likely in polymers (Fig. 17). If the chains themselves define the cavity traps, it is very reasonable that TSC spectra depend upon the morphology (or crystallinity) of PE and that the detrapping of electrons is closely related to the molecular-chain motions. Then, the detrapping may be a dual process arising from the thermal erosion of the trap by molecular motions plus the thermal excitation of the electron in the trap.[19]

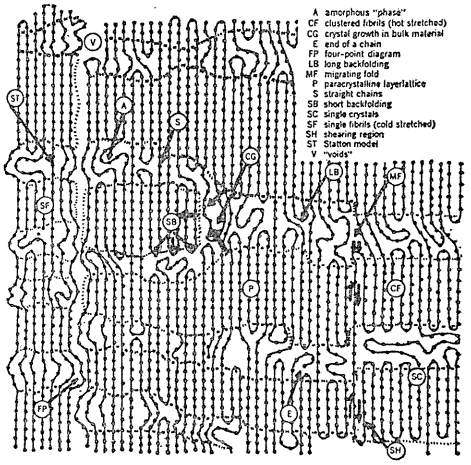

Fig. 17. Typical defects formed by local arrangements of polymer chains.

The C_6 peak appears in the β relaxation region (Fig. 16) and is enhanced with increasing vinyl acetate content. This suggests that the C_6 peak is due to the

polarization of the dipole of vinyl-acetate unit in the β relaxation region.

The TSC Ⅱ in EVA shows a current inversion at temperature T_0 ($T_0=273$K) following the C_6 peak. The total charge Q_d induced in the external circuit by the polarization of the dipoles up to T_0 is calculated from the area bound by the dipole TSC and the abscissa,

$$Q_d=S\int_{T_1}^{T_0}J_d(t)\,dt=\frac{S}{\beta}\int_{T_1}^{T_0}J_d(T)\,dT, \tag{31}$$

where S is the electrode area, $J_d(T)$ the TSC due to dipoles and β the heating rate. Since almost all dipoles are polarized up to T_0, Q_d is approximated by

$$Q_d/S=P_0(T_0)=n_d\mu_d^2F/3kT_0, \tag{32}$$

where n_d and μ_d are the concentration and the moment of the dipole, P is the polarization and k the Boltzmann constant. The total charge calculated from the second TSC spectra of EVA is plotted against the concentration of the vinyl acetate as shown in Fig. 18. Substituting $F=90$kV/cm, $T_0=273$ K into Eq. (32), we get $\mu_d=1.8$ D from the slope of a straight line in Fig. 18. This value agrees well with the 1.63–1.75 D obtained by Eidel'nant.[23] The magnitude of the inversion current is about 10^{-12} A/cm^2 and agrees well with value expected from Eq. (28).

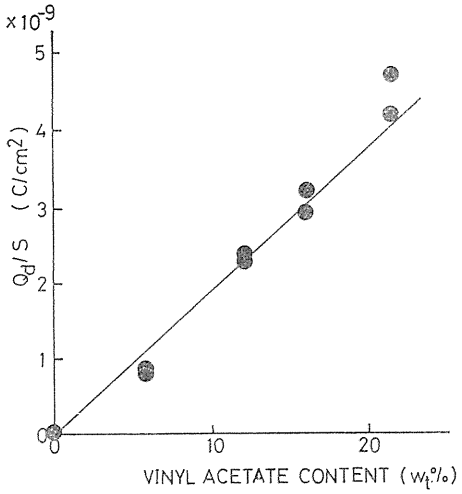

Fig. 18. Total charge Q_d induced by dipoles against the concentration of vinyl-acetate units.

4. 3. 3. Field dependence of TSC

The field dependence of TSC from HD-PE and LD-PE irradiated with X-rays is shown in Figs. 19 and 20. The TSC increases with the field in both HD-PE and LD-PE. For HD-PE, the peak temperature decreases with increasing field. Since C_1, C_4, C_5 and C_5' peaks are not clearly split in the high field region and the C_1 peaks is small, the exact evaluation of the change in peak temperature of these peaks is difficult. Therefore, the discussion will be limited to the C_2 and C_3 peaks.

The change of TSC peak temperatures with the applied field can be explained in terms of the lowering of barrier height by electric field as it occurs for instance in the Poole-Frenkel effect.[36] According to the conventional theory of TSC [§ 2. 2], the peak temperature T_m can be given by

$$\frac{B}{\beta}=\frac{E_t}{kT_m^2}\exp\left(\frac{E_t}{kT_m}\right). \tag{33}$$

From this relation, the small change in the peak temperature, ΔT_m, with that in the trap depth, ΔE_t, can be expressed by

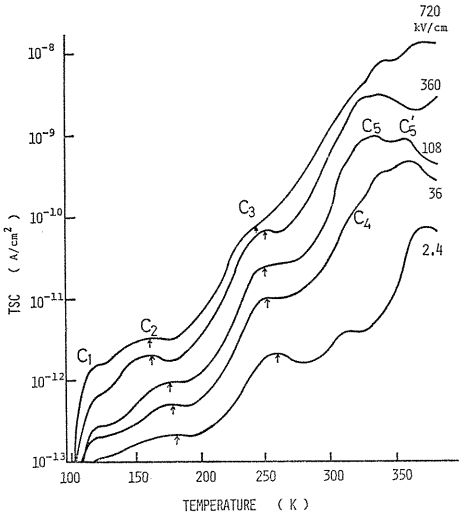

Fig. 19. Field dependence of TSC in HD-PE irradiated with X-rays.

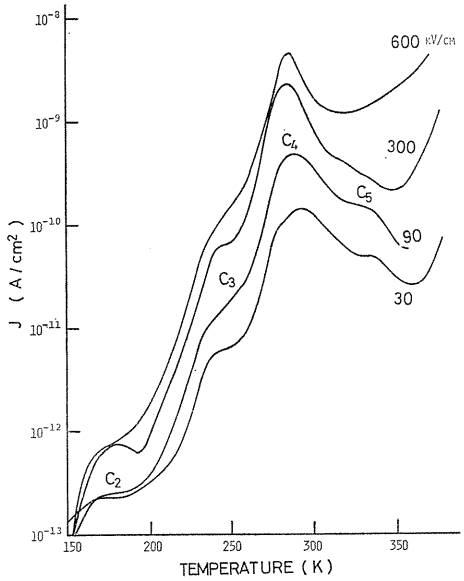

Fig. 20. Field dependence of TSC in LD-PE irradiated with X-rays.

$$\frac{\Delta E_t}{E_t}=\frac{\Delta T_m}{T_m}\left[1+1/\left(1+\frac{E_t}{kT_m}\right)\right]. \tag{34}$$

In our experiments, E_t/kT_m is much larger than the unity since T_m is 100–400 K and E_t estimated from the partial heating technique is 0.3–1.7 eV. Thus, Eq. (34) can be approximated by

$$\frac{\Delta E_t}{E_t}\simeq\frac{\Delta T_m}{T_m}. \tag{35}$$

Using this relation and the values of E_t estimated from a partial heating technique under the bias field of 108 kV/cm, 0.29 and 0.92 eV for C_2 and C_3 respectively, the change of E_t with the variation of an applied field can be estimated as shown in Fig. 21, where the trap depth decreases with an increasing field. This method is more convenient and accurate for evaluating a small change in E_t than the initial rise method.

The lowering of barrier height by electric field has often been explained in terms of the Poole-Frenkel mechanism. Assuming that the vacant trapping sites are charged, the trap depth E_t is given by

$$E_t=E_{t0}-\beta_{PF}\sqrt{F}, \tag{36}$$

where E_{t0} is the depth when the bias field is zero, F is the bias field, $\beta_{PF}=(e^3/\pi\varepsilon\varepsilon_0)^{1/2}$, e is the electron charge and ε is the relative dielectric constant. Applying this relation to the experimental results, we get from the slope of straight lines in Fig. 21,

$$\beta_{PF} \simeq 0.0016\text{eV}(\text{kV/cm})^{1/2} \quad \text{for } P_2$$
$$\simeq 0.0022\text{eV}/(\text{kV/cm})^{1/2} \quad \text{for } P_3$$

and thus

$$\varepsilon \simeq 220 \quad \text{for } P_2$$
$$\simeq 110 \quad \text{for } P_3.$$

These calculated values of ε are considerably higher than those reported for ε of polyethylene, which are around 2.3. The experimental results obtained cannot, therefore, be explained by the ordinary Poole-Frenkel mechanism.

If physical defects such as cavities, as has been suggested in the previous section, act as traps, the self-trapping mechanism is likely to occur. Garton and Parkman concluded that electrons were self-trapped in polyethylene.[38] In case of self-trapping, the effective trapping site charge which gives rise to a potential energy that acts back on an electron is expressed by

$$e(1/\varepsilon_\infty - 1/\varepsilon), \qquad (37)$$

where ε_∞ is the value of ε at very high frequency.[39] In such a case, β_{PF} is given by $[e^3(\varepsilon-\varepsilon_\infty)/\pi\varepsilon\varepsilon_\infty\varepsilon_0]^{1/2}$ and it is much smaller than β_{PF} in the ordinary Poole-Frenkel mechanism. Assuming that ε_∞ and ε of polyethylene are 2.28 and 2.30, respectively, we get $\beta_{PF}=0.0015$ and the apparent dielectric constant $\varepsilon\varepsilon_\infty/(\varepsilon-\varepsilon_\infty)$ is about 260. Thus the small experimental value of β_{PF} can be explained in terms of self-trapping.

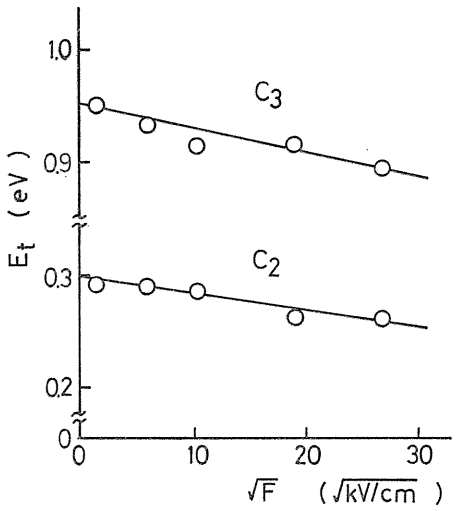

Fig. 21. Change in E_t with applied field in HD-PE.

In LD-PE, peak temperatures seem to remain unchanged. This may be attributed to the very small difference between ε_∞ and ε, if the Poole-Frenkel mechanism applied to the self-trapping holds in this case. The competition between the lowering of barrier height with field and the changes E_t with temperature steeper than in HD-PE may result in smaller changes in T_m.

4. 3. 4. Photo-stimulated detrapping current (PSDC) in polyethylene[40]

Since the TSC results are analysed with the assumption that trapping parameters are independent of temperature, difficulties may be encountered in their evaluation in case that some of them change with temperature. In such a case, the technique of photo-stimulated detrapping current (PSDC) which utilizes light energy to release trapped carriers isothermally is very powerful for analysing the nature of traps.

Figure 22 shows the obtained PSDC spectra for HD-PE (corrected for light

intensity) plotted against exciting photon energy. Curve A shows the PSDC spectrum observed just after the X-ray irradiation and curves B, C, D and E show the spectra after some of TSC peaks were thermally eliminated by heating the specimen up to 203, 273, 328 and 383 K respectively. As HD-PE without X-ray irradiation showed no PSDC, these spectra are due to trapped carriers introduced by X-ray irradiation. The PSDC peak around 1 eV disappears after heating the specimen up to 203 K and this thermal treatment also eliminates the C_1 and C_2 TSC peaks. Their disappearance suggests that the traps responsible for the C_1 and C_2 peaks are about 1 eV in depth. The thermal elimination of the C_3 peak reduces the PSDC above 1.5 eV by about one order, indicating that the trap depth for the C_3 peak is more than 1.5 eV. The disappearance of the PSDC above 4 eV after the thermal elimination of the C_4, C_5 and C_5' peaks also suggests that the traps for these peaks are more than 4 eV in depth.

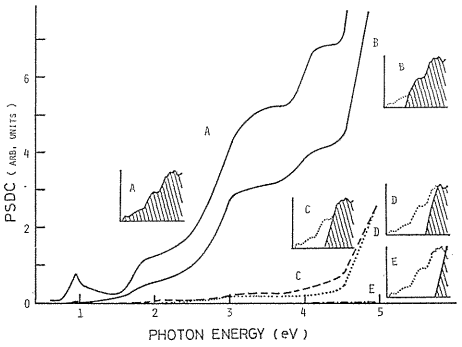

Fig. 22. RSDC spectra for HD-PE.

As shown in Fig. 15, the trap depths estimated from TSC experiments are about 0.3 eV (C_1 and C_2), 0.9 eV (C_3), and 1.4–1.7 eV (C_4, C_5 and C_5'). Trap depths in HD-PE estimated from TSC experiments have also been reported by other authors, for example, 0.35, 0.6 and 1.1 eV by Perlman and Unger[44] and 0.09, 0.17, 0.35 and 0.62 eV by Amakawa and Inuishi.[24] These values are much smaller than those obtained by PSDC experiments.

The trap depths estimated from PSDC experiments are those estimated at a constant temperature of 90 K where molecular motions are frozen up. On the other hand, those from TSC measurements are depths estimated at a higher and increasing temperature under the influence of molecular motions. Therefore, their difference may be attributed to the thermal change of traps which is caused mainly by molecular motions. This assumption is very reasonable if physical defects such as cavities are acting as traps and the carriers are released through thermal erosion of the traps themselves.

4. 3. 5. Effects of oxidation on TSC in PE

Figure 23 shows the effect of oxidation on TSC spectra of HD-PE. With increasing oxidation, a new C_5'' peak around 360 K increased and the remaining TSC peaks C_1–C_5 were reduced. Another new peak (C_3'') was observed only in slightly oxidized HD-PE (sample B). The apparent trap depth E_t was estimated by the partial heating method.[24] The resultant trap depth is plotted in Fig. 24 against the maximum temperature reached in each partial heating.

The oxidation products such as C=O groups have been reported to act as carrier traps.[20, 21] The enhancement of the C_5'' peak suggests the introduction of deep traps by oxidation. The decrease of TSC without X-ray irradiation by oxidation (Fig. 23) can be ascribed to the decrease of carrier mobility and / or the decrease of mobile carrier densities due to the increase of deep traps. Then, the decrease of the C_1, C_2, C_3, C_4 and C_5 peaks can also be ascribed to the retrapping of detrapped carriers by the deep traps and / or the decrease of trapped carriers

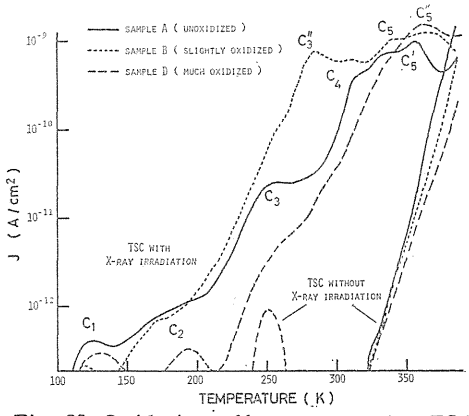

Fig. 23. Oxidation effects upon the TSC spectra of HD-PE.

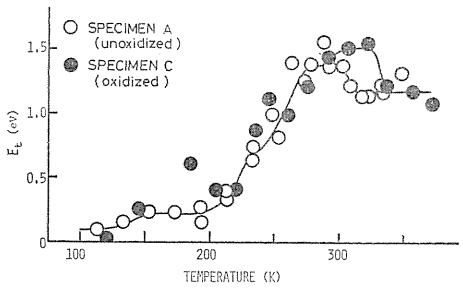

Fig. 24. Apparent trap depth E_t versus the maximum temperature reached in each partial heating for HD-PE.

due to the competition with the deep traps.

The C_3'' peak was observable only in slightly oxidized HD-PE (sample B) and was removed by further oxidation. As shown in Fig. 25, it also disappeared when the sample B was annealed at 383 K for an hour before X-ray irradiation. Therefore, the carrier trapping sites responsible for the C_3'' peak seem to be unstable intermediate products in the oxidation process.

Judging from the oxidation process of PE,[46] radicals or ozonides may be the trapping sites responsible for the C_3'' peak. ESR and infrared absorption measurements were carried out on sample B, sample B annealed at 383 K for an hour, and sample C. No ESR signal due to radicals could be detected, indicating less possibility of radicals being the trapping sites. Sample B has absorption bands of ozonides at 1054 and 1107 cm^{-1} and very weak absorption of carbonyl groups. Annealing of sample B reduces the absorption bands of ozonides and enhances the absorption band of aldehyde groups at about 1730 cm^{-1}. These facts seem to support the possibility of ozonides being the trapping sites. However, although precise quantitative estimation of ozonides is difficult, sample C, which exhibits no C_3'' peak seems to have more ozonides than sample B. Therefore, the trapping sites for the C_3'' peak seem to be neither radicals nor ozonides. However, the mechanism of ozonization of polymers is somewhat complicated and many other intermediate products such as molozonides and peroxides have been reported to exist in the oxidation process.[47~49] Some of them may be the trapping sites for the C_3'' peak.

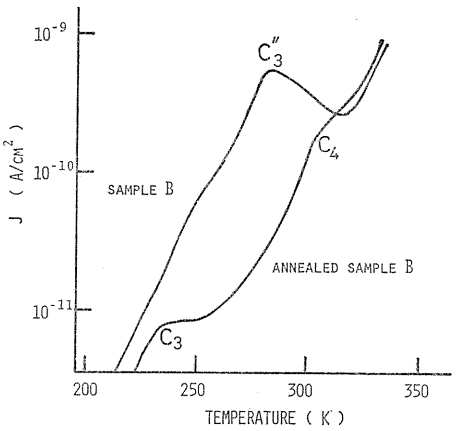

Fig. 25. Effect of annealing upon the C_3'' peak.

The deep trapping sites introduced responsible for the C_5'' peak are considered to be stable oxidation products such as carbonyl groups, as the annealing of much oxidized HD-PE does not influence the TSC spectra. This is supported by the fact that the infrared absorption spectrum of much oxidized HD-PE is not changed by annealing.

Similar oxidation effect was observed for LD-PE. The TSC spectrum of oxidized LD-PE is shown in Fig. 26, together with that of non-oxidized LD-PE. Oxidation reduced the C_1–C_5 peaks and enhanced a new peak (C_5'') around 310 K. The apparent trap depth E_t estimated from the initial rise of the partial heating curve[24] is shown in Fig. 27.

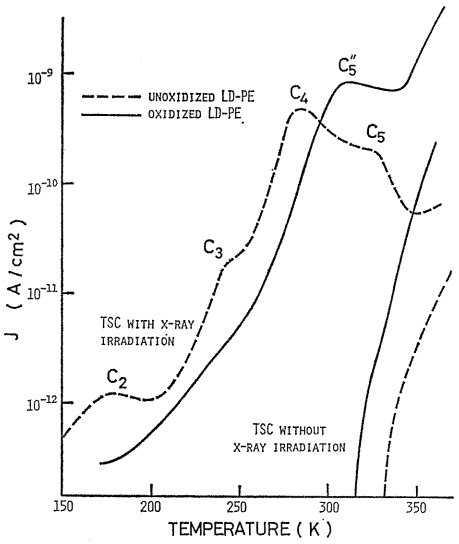

Fig. 26. Oxidation effects upon the the TSC spectra of LD-PE.

It should be noted that the peak temperature of the C_5'' peak enhanced by oxidation depends upon the morphology (or the crystallinity) of PE. The C_5'' peak appears at 360 K in HD-PE, and at 310K in LD-PE. There is also a remarkable difference in the TSC without X-ray irradiation between HD-PE and LD-PE. The TSC without X-ray irradiation of HD-PE was reduced by oxidation, while that of LD-PE was enhanced as shown in Figs. 23 and 26. Such differences can be clearly observed in the isothermal current characteristics.[50, 51] Figure 28 shows the oxidation dependence of the isothermal current and the mobility in PE. The values of mobility were estimated from the transient current peaks on the basis of the transient SCLC theory.[52] The change in current density is in a good agreement with the change in mobility, suggesting that the former is caused by the latter. A qualitative explanation of the opposing oxidation effects upon the mobility between HD-PE and LD-PE was given, based on the assumption that carbonyl groups introduced in the amorphous regions of PE act as hopping centers, whereas oxidation products introduced in the crystalline surface regions become deep traps.[53] In LD-PE with a high portion of amorphous parts, the carrier mobility is enhanced by the hopping centers due to C=O groups in the amorphous part. On the other hand, the C=O groups (deep traps) in the crystalline surface region effectively reduce the carrier mobility in HD-PE with a high crystallinity because electrons injected from the electrode must move in HD-PE through the crystalline parts.

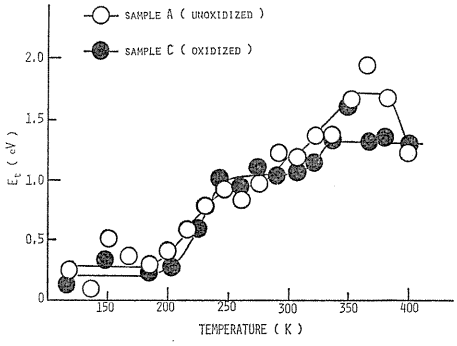

Fig. 27. Apparent trap depth E_t versus the maximum temperature reached in each partial heating for LD-PE.

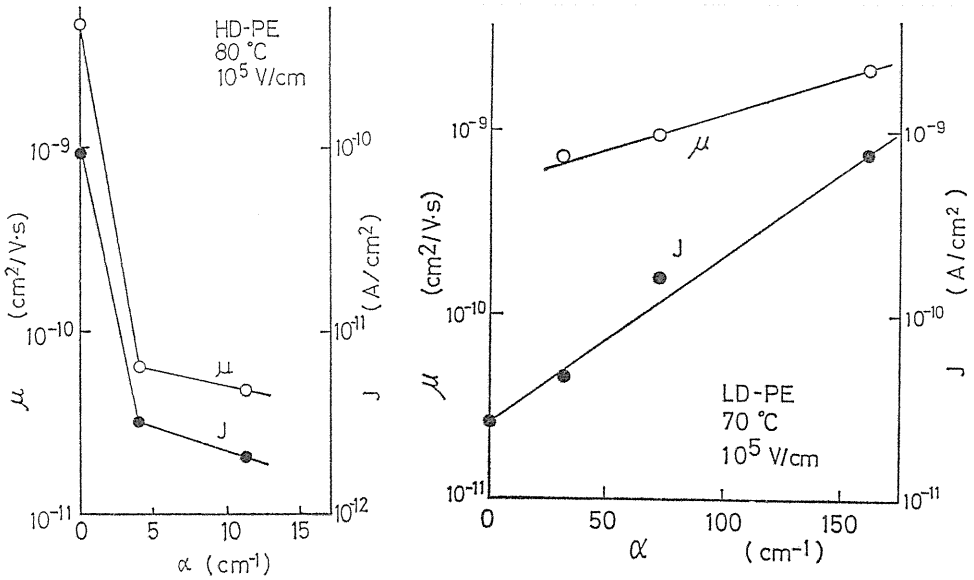

Fig. 28. Oxidation effects upon the current and the mobility in PE.

According to Exstrom and Willard,[31] the depth of cavity trap depends upon the size of cavity and it is approximately proportional to R_0^{-2}, where R_0 is the cavity radius. Assuming that the C=O trap is ascribed to the cavity created by a C=O group in the PE chain, it is reasonable that the C=O trap in the crystalline surface regions is deeper since the size of the C=O cavity is smaller in the crystal surface region tightly bounded by crystallites than in the free amorphous region.

4. 3. 6. Effcts of γ-irradiation and cross-linking.

In general, the γ-irradiation in air promotes the oxidation of PE.[54, 55] Therefore, to eliminate the oxidation effect, the specimen was irradiated with γ-rays in vacuum. After the irradiation, it was annealed for an hour in a vacuum at 393 K under a short circuit condition, in order to remove carriers generated by the γ-ray excitation.

Figure 29 shows the resultant TSC spectra in γ-irradiated HD-PE. The TSC with X-ray irradiation has a new peak C_7 around 390 K and in the low temperature region it is much smaller than that of HD-PE without γ-irradiation. The TSC without X-ray irradiation is also much smaller than that of virgin HD-PE. These phenomena are very similar to those in oxidised HD-PE. Therefore, γ-ray irra-

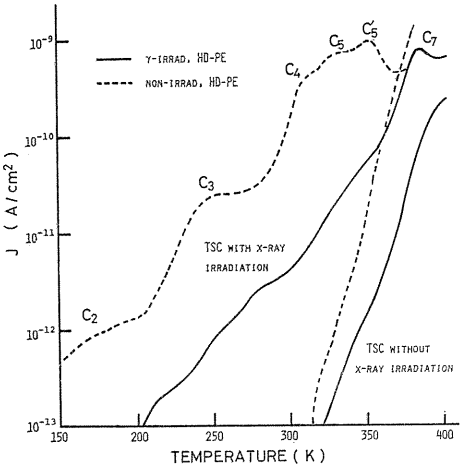

Fig. 29. TSC spectra for γ-irradiated HD-PE.

diation in vacuum seems to introduce deep traps into PE. The possible origins of the deep traps introduced by the γ-irradiation are radiation defects such as radicals, cross-links, chain scission, double bonds, etc. Takai et al.[41] reported on the basis of PSDC analysis that the cross-link due to the γ-irradiation in vacuum act as a deep trap.

Figure 30 shows a typical X-ray induced TSC in XL-PE. The cross-linking introduces a new TSC peak (C_7) around 360 K and it reduces the TSC peaks C_1–C_5. These suggest that cross-link points act as deep traps like oxidation products in HD-PE.

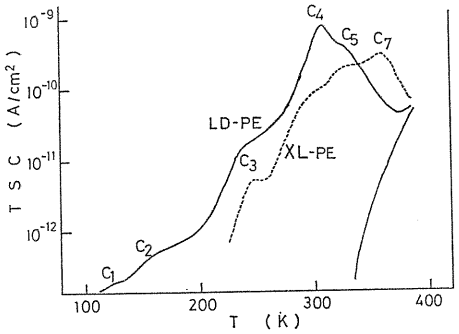

Fig. 30. X-ray induced TSC spectra of cross-linked PE (XL-PE).

4. 3. 7. Energy level diagram for PE

In the previous sections, we clarified the natures and the origins of carrier traps in PE. These results are summarized in Table 5.

Polyethylene is a long-chain organic polymer. The intermolecular bonding is weak and molecular and the overlap integral between adjacent chains is about 0.001eV.[56, 57] For this reason alone the usual concepts of the band theory would not appear very useful. However, the intramolecular bonding is strong and covalent and so the band scheme is derived for a PE chain. Recently, the theoretical calculations of the energy band structure of PE have been reported by many authors.[26, 58~62]

Table 5. Carrier traps in polyethylene.

TSC		Traps corresponding to TSC peaks		
Peak	Peak Temperature	Trap Depth	Region	Origin
C_1	~130 K	0.1–0.3 eV		Defect
C_2	~200 (HD-PE) ~180 (LD-PE)	0.3 0.24	Lamellar Surface (HD-PE) Amorphous Region (LD-PE)	
C_3	~250	0.8–1.0	Amorphous Region	
C_4	230~310	1.0–1.4	Amorphous-Crystalline Interface	
C_5	~330	1.2–1.4	Crystalline Region	
C'_5	~350 (HD-PE)	1.7		
C''_3	~280 (HD-PE)		Amorphous	Unstable Oxidation Products
C''_5	~360 (HD-PE) ~310 (LD-PE)	1.4	Amorphous-Crystalline Int. Amorphous	Stable Oxidation Products
C_7	~390 (HD-PE) ~320 (LD-PE)	1.0	Amorphous	Cross-link

They are based on the crystal orbital theory at various levels approximation; i. e. EHT (Extended Huckel Theory)[63], CNDO (Complete Neglect of Differential Overlap),[59,66] INDO (Intermediate Neglect of Differential Overlap),[62] MINDO (Modified INDO)[65,66] and Abinitio.[62,67] The resultant theoretical band structures are summarized in Fig. 31, together with the band structure estimated

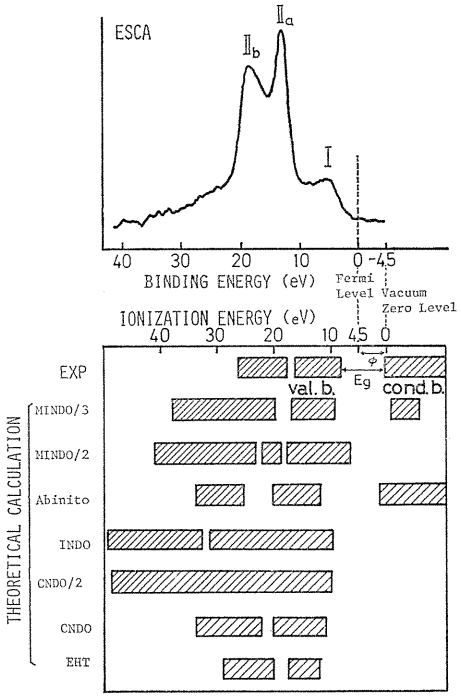

Fig. 31. Band structure of polyethylene.

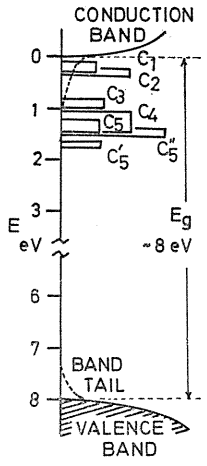

Fig. 32. Energy level diagram of carrier traps in polyethylene.

experimentally by the ESCA,[27,68] on the assumption of the work function (4.5eV) of PE.[69] The energy gap between the valence band and the conduction band calculated by MINDO/3 is 7.6 eV and it is in almost perfect agreement with ESCA experiment (7.7 eV).[68] The band gap of PE has been also estimated as about 8 eV from UPS (Ultraviolet Photoelectron Spectroscopy)[69] and UV absorption[70], and as 8.8 eV from the UV photoconduction.[71] The UPS experiment[72] also revealed that the conduction band of PE extends up to about 7 eV above the effective vacuum level.

Considering the above band structure of PE and the values of trap depth in Table 5, we obtain the energy level diagram of PE as shown in Fig. 32.

4. 4. Conclusions

The present chapter dealed with the X-ray induced TSC from various polyethylenes, that is HD-PE, MD-PE, LD-PE, EVA and XL-PE. The X-ray induced TSC technique is very useful to distinguish between the TSC peak due to trapped carriers and that due to dipoles. Much information about the natures and the origins

of carrier traps in PE has been obtained.

Non-treated PE showed five or six TSC peaks due to trapped carriers, designated by C_1 to C_5 (C_5') in ascending order of temperature. This suggests the existence of five or six kinds of carrier traps. The release of carriers from traps is closely related to the onset of molecular motions in PE. The C_2 peak appears in the γ relaxation region. The C_3 peak in the β relaxation region is ascribed to the amorphous part, and the traps responsible for the C_4 peak may lie in the amorphous-crystalline boundary, i. e. the folded region. The C_5 and C_5' peaks corresponding to the α and α' relaxation are associated with the crystalline region. The origins of these traps are concluded to be physical defects such as formed by local arrangements of molecular chains.

The field dependence of peak temperatures in HD-PE suggests the reduction of trap depth with field. The relatively small change in trap depth can be explained in terms of the Poole-Frenkel effect applied to the self trapping. The comparison between apparent trap depths obtained from TSC and PSDC revealed that the erosion of traps by molecular motions plays an important role in the reduction of the trap depth. These results are all suggestive of cavity traps.

The oxidation products such as C=O groups and cross-linking points were proved to act as carrier traps. The C=O group attached to a PE chain or the cross-linking between adjacent PE chains may distort the local arrangement of molecular chains and introduce a cavity pictured as an irregular space. Such cavities are probably the origins of the carrier traps due to the C=O group and the cross-linking point.

The natures and the origins of carrier traps in PE clarified in this chapter are summarized in Table 5 and also in Fig. 32.

5. X-ray Induced TL from Polyethylene

5. 1. Introduction

In the previous chapter, we have revealed that polyethylene has many kinds of carrier traps possibly due to physical defects and that the detrapping of carriers are closely related to molecular motions. However, since TSC from polyethylene in the low temperature region is very small presumably because of low carrier mobility, it is difficult sometimes to analyse the natures of the corresponding traps. In addition to the TSC measurements, it is of a great help to measure the thermoluminescence which is dominant in the low temperature region. Thermoluminescence from polyethylene has been widely investigated[18, 19, 32, 73~75] and carrier trapping sites and luminescence centers have been ascribed to various physical and chemical structures.

In this chapter, the thermoluminescence (TL) from polyethylene has been investigated, especially that from HD-PE in which the effects of oxidation on TL are remarkable. The location of carrier traps, especially those corresponding to the C_1 and C_2 TSC peaks in the preceding chapter, has been determined. The changes of traps and luminescence centers by oxidation have been discussed.

5. 2. Experimental

Specimens were films of the same LD-PE, HD-PE and EVA-4 as in the TSC

experiments. Some of them were oxidized at room temperature by exposure to an ozone atmosphere produced by the gas discharge in oxygen. Table 6 is the list of specimens, where the oxidizing time indicates the duration of exposure of the specimen to an ozone atmosphere. The extent of oxidation was estimated from the infrared absorption of the main carbonyl stretching at about 1720 cm^{-1}.

Table 6. List of specimens.

specimen		oxidizing time	absorption coefficient at about 1720cm^{-1}
LD-PE	A	0 mim	—
	B	60	14 cm^{-1}
	C	100	32
	D	200	46
	E	1310	412
	F	2030	1640
HD-PE	A	0	—
	B	60	21
	C	1310	360
EVA-4			

5. 3. *Experimental Results*

Figures 33, 34 and 35 show the observed TL spectra from HD-PE, LD-PE and EVA-4, together with their TSC spectra. The TL peaks, $H_1(L_1)$, $H_2(L_2)$ and $H_3(L_3)$ corresponds well to the TSC peaks, C_1, C_2 and C_3, respectively. The $H_1(L_1)$, $H_2(L_2)$ $H_3(L_3)$ peaks in PE decrease with increasing oxidation and new peaks $H_4(L_4)$ and $H_5(L_5)$ appear. The oxidation of HD-PE effectively depresses the H_1 and H_3 peaks and makes the H_2 peak observable. The oxidation effects can

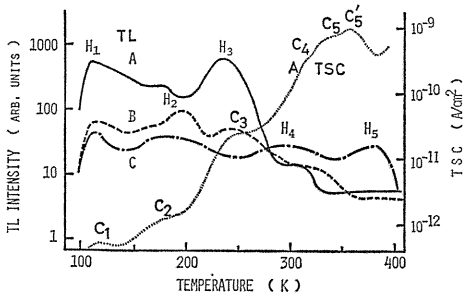

Fig. 33. TL spectra of HD-PE, together with the TSC spectrum. Curve A, B and C show the TL spectra of specimens A, B and C, respectively.

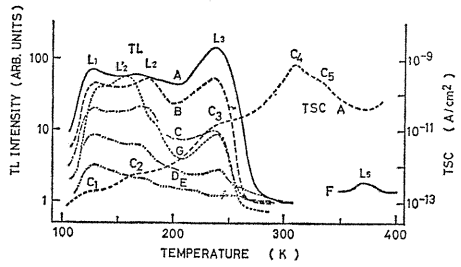

Fig. 34. TL spectra of LD-PE, together with the TSC spectrum. Curve A, B, C, D, E and F show the TL from specimens A, B, C, D, E and F, respectively. Curve G shows the TL from unoxidized LD-PE in oxygen atmosphere.

be explained by the introduction of deep traps by oxidation as mentioned in § 4. 3. 5.

In Figs. 36 and 37 the apparent trap depths estimated from the initial slope of each TL curve in the ln (TL intensity)–$1/T$ plot are plotted against the maximum temperature reached in each partial heating.[24] These values are similar to those obtained from the TSC experiments. The

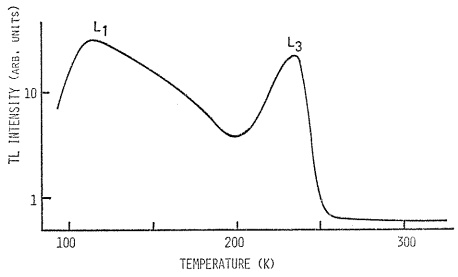

Fig. 35. TL spectra of EVA-4.

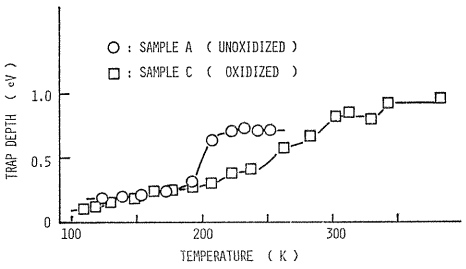

Fig. 36. Apparent trap depth E_t for HD-PE obtained from the partial heating.

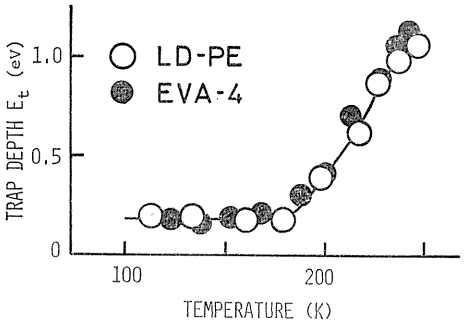

Fig. 37. Apparent trap depth E_t obtained from the partial heating.

difference in trap depth between unoxidized HD-PE : A and oxidized HD-PE : C in temperature range of 190–250K is considered to be due to the disappearance of the H_3 peak in oxidized HD-PE. The apparent trap depth for the H_1 and H_2 peaks seems to be unaffected by oxidation.

TL can be optically bleached. After X-ray irradiation, a sample was illuminated for 30 minutes at 90 K by a light which was filtered with a sharp-cut low-pass glass filter. Then the TL was measured. In Figs. 38 and 39, the intensity of each TL peak is plotted against the cut-off wavelength of the filter used in the bleaching experiment. TL peaks of unoxidized LD-PE and HD-PE were easily bleached by lights with wavelength $\lambda > 670$ nm, but those of oxidized HD-PE were bleached by lights with $\lambda < 450$ nm. Yet the H_5 peak could not be bleached even by a light $\lambda \simeq 250$ nm. The trap depth estimated from the optical bleaching experiments responsible for TL peaks of unoxidized HD-PE seems to be less than 1.9 eV and that of oxidized HD-PE to be about 3 eV.

In order to clarify the mechanism of luminescence, spectral distribution of TL peaks were obtained with interference filter whose band width was 10–20 nm. Each filter was placed between the quartz window and the photomultiplier tube. The results are shown in Figs. 40 and 41. The spectra for unoxidized polyethylene show two components, one being 300–350 nm, the other 450–550 nm. On the other hand, all TL peaks of the oxidized HD-PE have the same spectral distribution with only one peak at 550 nm.

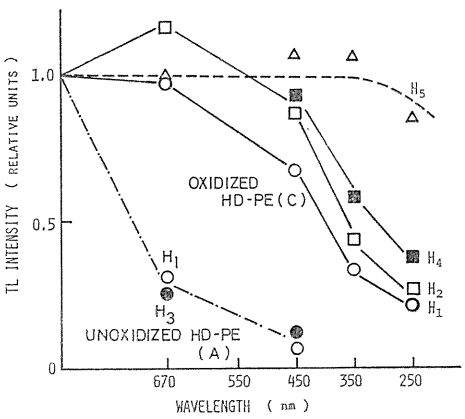

Fig. 38. TL intensity for HD-PE after optical bleaching versus cut-off wavelength of the sharp-cut filter used.

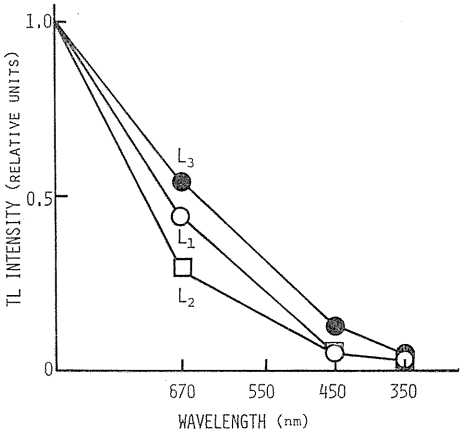

Fig. 39. TL intensity for LD-PE after optical bleaching versus cut-off wavelength of the sharp-cut filter used.

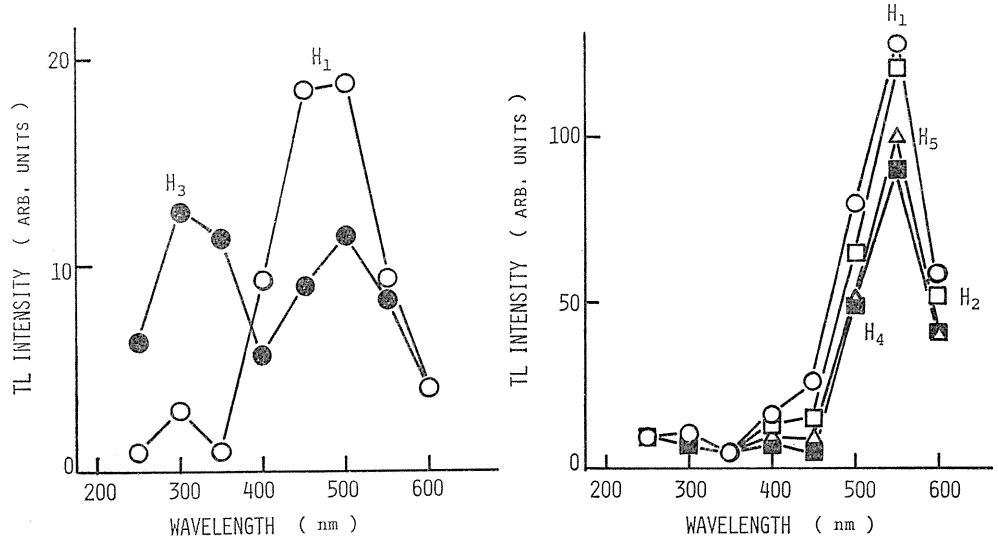

Fig. 40. Spectral distribution of TL peaks from HD-PE.

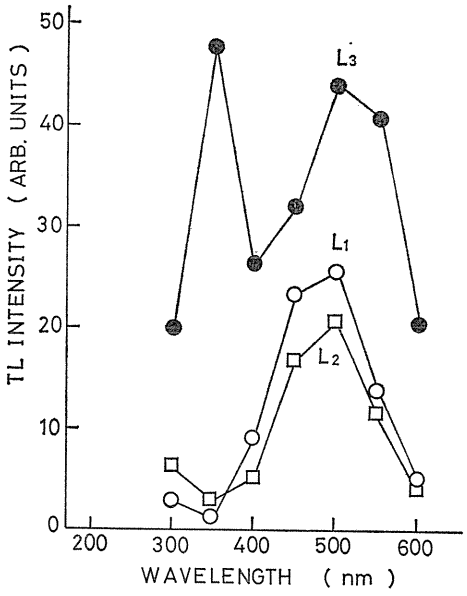

Fig. 41. Spectral distribution of TL peaks from LD-PE (specimen A: unoxidized).

5. 4. Discussion

TL from γ-irradiated HD-PE was reported by Blake et al.[18] and their results are similar to those obtained here. They attributed five TL peaks to the following phenomena: 110 K-γ-relaxation; 160 K-trapping by molecular oxygen; 200 K-relaxation intermediate in temperature between the γ- and the β-relaxations; 230 K-β-relaxation; 310 K-α-relaxation. It can be concluded that the traps responsible for the L_3 and H_3 peaks lie in the amorphous regions for the following reasons; (i) they appear in the temperature region of the β-relaxation assigned to the amorphous parts,[30] (ii) they show a greater sensitivity to oxidation which occurs in the amorphous regions than the other peaks. When an unoxidized sample was set in an oxygen atmosphere of 100 Torr, its TL spectrum showed a new peak between the $H_1(L_1)$ and $H_2(L_2)$ peaks due to molecular oxygen. Neither the $H_1(L_1)$ nor the $H_2(L_2)$ peak is, therefore, related to molecular oxygen. Nara et al.[76] examined the molecular motions in polyethylene through ESR experiments and compared their data with those by Kakizaki and Hideshima for dielectric relaxation[77]. According to Nara et al., molecular motion around 200 K for HD-PE is associated with the γ-dispersion in lamellar surfaces and that around 180 K for LD-PE corresponds to the γ-dispersion in the amorphous phase, i. e. local mode relaxation.

Figure 33 shows that of peaks H_1, H_2 and H_3, the H_2 peak has the lowest decay rate and it seems to be related to the crystalline regions where oxidation is difficult to occur. The corresponding TL peak (L_2) for LD-PE decayed faster than L_1 peak and it can be considered to be associated with amorphous regions. It can be, therefore, concluded that the traps responsible for the H_2 peak lie in lamellar surfaces and those for the L_2 peak in amorphous regions. It is not clear whether or not the H_1 and L_1 peaks are associated with a slight motion of molecules (δ-dispersion) in the amorphous phase, a motion that Nara et al. considered to correspond to the free radical decay around 120 K.[76] Since with oxidation the

H_1 and L_1 peaks decay at a considerable rate, traps responsible for them may lie in the amorphous regions.

The enhancement of the H_4, H_5 and L_5 peaks is note worthy. These peaks may be closely related to the crystalline part, because the corresponding TL peaks for LD-PE are very small. The increase of the H_4 peak by oxidation may be ascribed to the increase of deep traps due to oxidation products. It is also note worthy that the H_5 peak, unlike the other peaks, appears even without X-ray irradiation (Fig. 42). Its magnitude depends only on the extent of oxidation. Therefore, the H_5 and L_5 peaks do not seem to be due to trapped carriers introduced

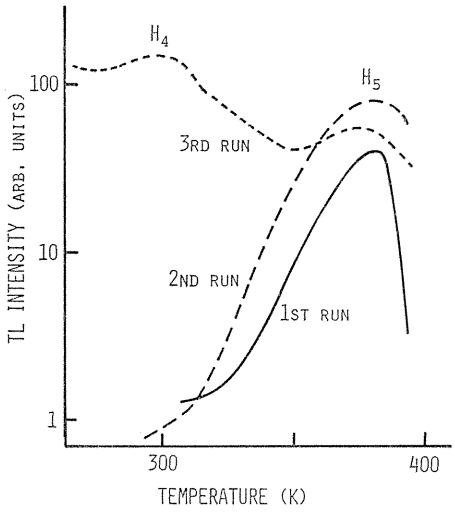

Fig. 42. TL H_5 peak from oxidized HD-PE (specimen C);
1st run: TL without X-ray irradiation,
2nd run: TL without x-ray irradiation obtained after the lst run,
3rd run: TL with X-ray irradiation obtained after the 2nd run.

by X-ray irradiation. These peaks seem to correspond to tha P_a peak in γ-irradiated polyethylene observed by Nakamura et al.[78]

The trap depth estimated from the partial heating (Figs. 36 and 37) is less than 1.0 eV, whereas the optical trap depth estimated from the optical bleaching (Figs. 38 and 39) seems to be much larger. For example, the traps for the H_1 peak of the oxidized HD-PE show 0.15–0.2 eV thermally but about 3 eV optically. This suggests that detrapping is predominantly due to thermal erosion of traps by molecular motions and not only to thermal escape from traps.

The spectral distribution of the unoxidized HD-PE and LD-PE shown in Figs. 40 and 41 is almost the same as that of γ-irradiated polyethylene obtained by Charlesby and Partridge.[32] The spectra of photoluminescence from HD-PE excited by a light with $\lambda=280$ nm at 90 K and room temperature showed two components, one being 300–350 nm, the other 450–550 nm. The former dose not vary with temperature but the latter can not be observed at room temperature. Charlesby and Partridge[32] and Somersall et al.[79] showed that below 110 K the phosphorescence intensity from polyethylene was constant but became very weak above 110 K. Thus the H_1 and L_1 peaks of unoxidized polyethylene are mainly due to phosphorescence, while the H_3 and L_3 peaks result from both phosphorescence and fluorescence. The spectral distribution of all TL peaks of oxidized HD-PE is the same and differ from that of unoxidized specimen. This shows that oxidation changes the

dominant luminescence centers responsible for TL peaks.

The quenching of the TL peaks by oxidation may be caused not only by the introduction of deep traps, but also by the lowering of the TL efficiency through the change of luminescence centers and / or the change of trap centers (the deepening of the optical trap depth) by oxidation. The increase of deep traps responsible for the H_4 peak, however, may also reduce the H_1, H_2 and H_3 peaks, if the detrapped electrons responsible for the TL peaks are captured by deep traps before reaching luminescence centers.

5. 5. Conclusions

The TL from polyethylene and its oxidation effects have been investigated. All TL peaks except H_5 and L_5 are associated with trapped carriers. The $H_1(L_1)$, $H_2(L_2)$ and $H_3(L_3)$ peaks are reduced by oxidation, while the H_4 peak is enhanced by it.

It can be concluded that the traps responsible for the H_3 and L_3 peaks lie in amorphous regions, and those responsible for the H_2 and L_2 peaks in amorphous regions and lamellar surfaces, respectively. Those responsible for the H_1 and L_1 peaks seem to be in amorphous regions and those responsible for the H_4 peak seem to be introduced by oxidation into the crystalline regions or the crystalline-amorphous interfaces.

The detrapping of carriers may be closely related to the thermal erosion of the trap by molecular motions. The TL spectra revealed that oxidation changes luminescence centers. The oxidation induced quenching of the TL peaks in the low temperature region may be caused not only by the introduction of deep traps, but also by the change of luminescence center and / or traps.

6. X-ray Induced TSC in Polyvinylidene Fluoride

6. 1. Introduction

In recent years, polyvinylidene fluoride (PVDF) has received considerable attention because of its piezoelectricity[80], pyroelectricity and high dielectric constant.[81] Moreover, the crystal of PVDF has at least three distinct polymorphs called the α, β and γ phases.[82] The α-phase has a herical conformation and dipoles are cancelled out in a unit cell. On the other hand, the β-phase has a planar zigzag type conformation and has large dipole moment perpendicular to the c-axis which results in spontaneous polarization. Recently, the existence of the polar α-phase structure has been pointed out.[83,84] Morphologically, PVDF is one of the interesting polymers.

It was generally believed that high piezoelectric coefficients of PVDF were due to the spontaneous polarization of β-PVDF.[85] Recently, however, several authors[86~89] have pointed out that the piezo- and pyroelectricity of PVDF is rather due to trapped charges (space charge) near the positive electrode. Many reports have been published on the origin of piezoelectlicity of PVDF.[90~95] However, we have still no clear understanding of the origin of piezoelectricity. The anomalous high value of the dielectric constant at high temperatures and low frequencies has also been attributed to space charge.[96] Space charge is closely related to carrier traps. It is strongly required to understand the natures and the

origins of carrier traps in PVDF.

In this chapter, carrier traps in PVDF have been studied by using the X-ray induced TSC technique.[97]

6. 2. Experimental

Specimens were unstretched, biaxially stretched and uniaxially stretched PVDF films (KF Polymer, Kureha Chemical Industries) of thickness 6–100 μm. All specimens used are summarized in Table 7. The experimental procedures of TSC were the same as in § 3. 3. 1.

Table 7. List of specimens.

Specimen	Thickness	Stretching	Crystalline phase
A	35μm	Unstretched	α
B	50	Unstretched	α
C	100	Unstretched	α
D	6	Biaxially stretched	$\alpha+\beta$
E	25	Biaxially stretched	$\alpha+\beta$
F	17	Uniaxially stretched	β

6. 3. Experimental Results

Figures 43, 44 and 45 show typical TSC spectra obtained under the bias field of ca. 90 KV/cm. TSC with X-ray irradiation in unstretched film (B) shows a large TSC peak around 330K. The difference between TSC with and without X-ray irradiation in both biaxially and uniaxially stretched films (D, E and F) is less clear than in unstretched ones. While unstretched films (A, B and C) show three peaks designated C_1, C_2 and C_3 in ascending order of temperature, the other specimens show only to split peaks, C_1 and C_2. These two peaks show no change with X-ray irradiation. TSC above 370K has a complicated structure.

Figure 46 shows the field dependence of the C_3 peak in unstretched film (B). The complicated behavior of this peak suggests that it is composed of two TSC peaks, i. e., C_3' and C_3'' peaks. The C_3' peak exhibits a remarkable peak temperature dependence on an applied field, while the C_3'' peak seems independent of it. The situation is more clear in the case of an annealed specimen, as shown in Fig. 47. Annealing was carried out for an hour at 423 K in vacuum.

Figure 48 shows the apparent trap depth estimated by the initial rise method.[24] The apparent trap depths are about 1eV for both C_3' and C_3'' peaks.

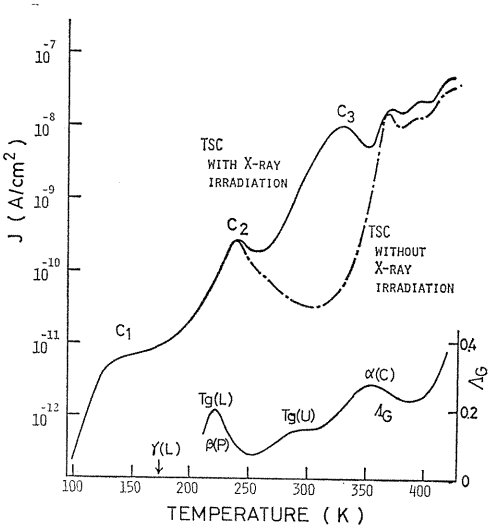

Fig. 43. TSC spectra of unstretched film, α-type PVDF(A) under a field of 90 kV/cm, together with the mechanical loss curve (Δ_G).[101]

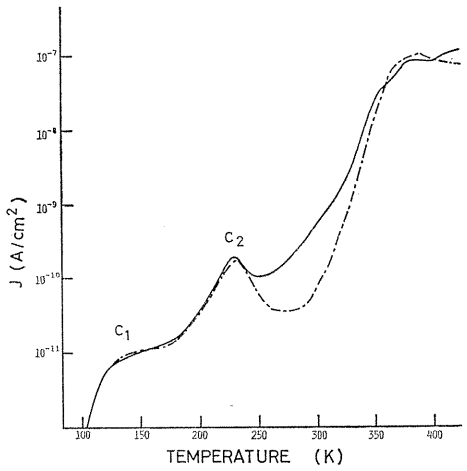

Fig. 44. TSC spectra of biaxially stretched PVDF film (E) under a field of 90 kV/cm.

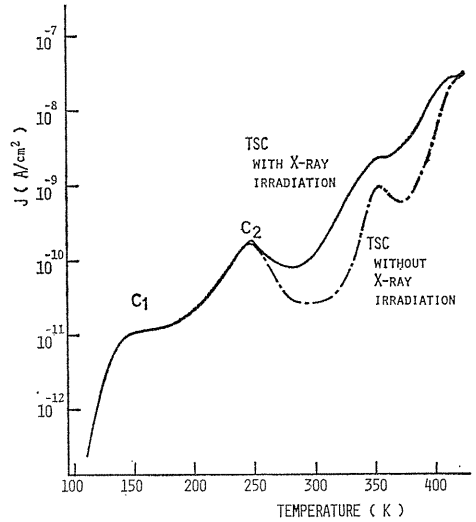

Fig. 45. TSC spectra of uniaxially stretched film (F), β-type PVDF under a field of 90 kV/cm.

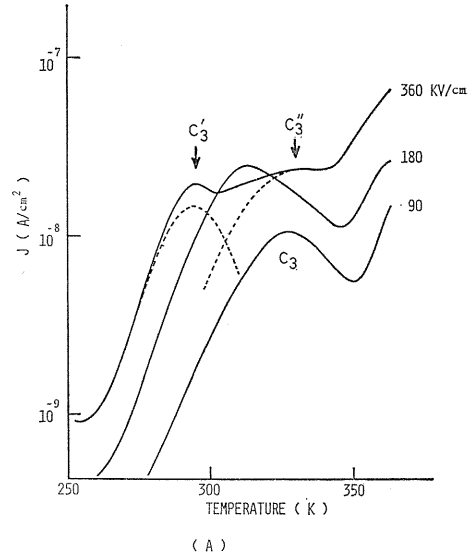

Fig. 46. Field dependence of the C_3 peak in the unstretched α-type PVDF.

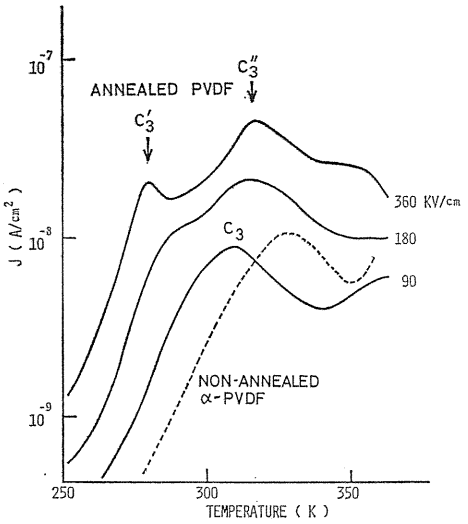

Fig. 47. Field dependence of the C_3 peak in annealed unstretched film (annealed B).

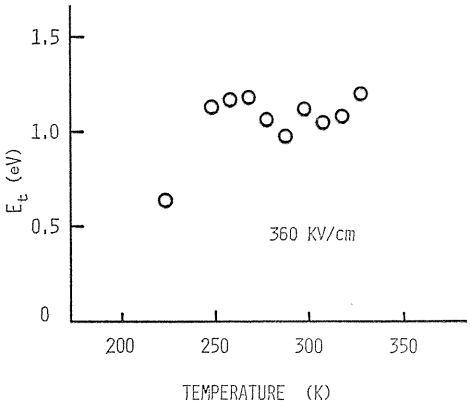

Fig. 48. Apparent trap depth E_t for the C_3 peak plotted against the maximum temperature reached in each partial heating.

6. 4. Discussion

TSC spectra from PVDF show three split peaks below ca. 360 K. TSC above 360 K has a complicated structure and does not exhibit marked dependence on X-ray irradiation. Therefore, TSC above 360 K is not discussed further.

The C_1 and C_2 peaks are independent of X-ray-irradiation. They increase linearly with increasing applied field. Moreover, their peak temperatures correspond well to the temperatures at which the γ and β relaxations in the amorphous region occur[98] (Fig. 43). These suggest that the C_1 and C_2 peaks are due to dipole orientation in amorphous regions.

The large TSC peak, C_3, around 330 K appears only in the TSC spectrum from the specimen irradiated with X-ray. This suggests that the C_3 peak is due to trapped carriers and that an abundance of carrier traps exist in PVDF. Furthermore, the C_3 peak explicitly appears only in the unstretched films (A–C) which are rich in the crystalline phase and consequently it is ascribable to the carrier traps in the crystalline phase and / or on its surface. The stretching of PVDF, which decreases the α-phase and increase the β-phase, reduces the C_3 peak and does not introduce any other explicit peaks. However, from the results of the radiation-induced conduction experiments, it seems that the β-type PVDF also contains a certain amount of carrier traps in the α-crystalline phase and / or on its surface.[95] The carrier detrapping in the β-type PVDF occurs at a temperature about 15 K higher than in the case of the α-type PVDF. Hence, the β-type PVDF may not exhibit any explicit TSC peak due to trapped carriers because of its high dark conductivity in the high temperature range.

As shown in Figs. 46 and 47 the C_3 peak is composed of the C_3' and C_3'' peaks and this suggests that at least two kinds of carrier traps are responsible for the

C_3 peak. Both these traps have apparent trap depth of about 1 eV.

It has been pointed out that many TSC peaks in polymers reflect relaxations at very low frequencies.[29] Takamatsu and Fukada reported a TSC peak around 340 K from an unstretched α-type PVDF thermoelectret and considered it to correspond to the relaxation around 340 K at 110 Hz, which has been ascribed to the α-relaxation in the α-crystalline phase by some authors.[90, 99, 100] Annealing a specimen for an hour at 423 K lowered the temperature of the C_3' and C_3'' peaks by about 15 K (Fig. 47), whereas it elevated the temperature of the dielectric loss peak around 350 K at 100 Hz and its peak temperature at lower frequencies deviates from the TSC peak temperature of 330 K. These suggest that the C_3 peak is less likely to this relaxation. Recently, however, Boyer summarized the relaxation temperatures for PVDF and concluded that the true crystalline phase relaxation at 1 Hz occurred around 350 K.[101] If this is the case, the C_3 peak possibly corresponds to this relaxation in the crystalline phase.

There is a remarkable difference in the field dependence between the C_3' and C_3'' peaks. The C_3' peak shifts to a lower temperature with increasing bias field, but the C_3'' peak does not. The lowering of the peak temperature suggests the reduction in the trap depth with bias field, such as the Pool-Frenkel effect.[36,37] The shift of the C_3' peak temperature is quantitatively explained from the Poole-Frenkel effect with the relative dielectric constant $\varepsilon=10$.

Figures 49 and 50 show the change in the TSC spectra with the temperature at which X-rays were irradiated. The experimental procedures are the same as

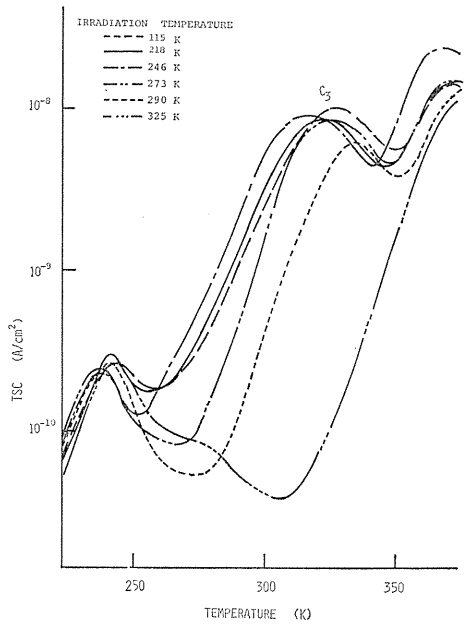

Fig. 49. Dependence of the C_3 peak under a field of 90 kV/cm on the temperature of X-ray irradiation (unstretched film B).

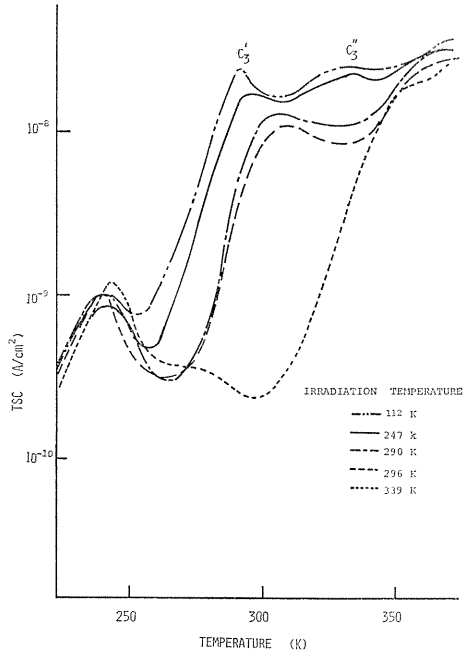

Fig. 50. Dependence of the C_3' and C_3'' peaks under a field of 360 kV/cm on the temperature of X-ray irradiation (unstretched film B).

mentioned in § 3. 3. 1 except that the specimen was irradiated at a certain temperature above 90 K and cooled down just after the irradiation. The irradiation was carried out under the short-circuited conditon.

As shown in Fig. 49 the C_3 peak is eroded from its low temperature side with increasing irradiation temperature, suggesting that the traps responsible for the low temperature side of the C_3 peak release carriers more easily than those for the high temperature side.

At a high bias field of 360 kV/cm, on the other hand, the high temperature peak (C_3'') is reduced more easily than the lower temperature peak (C_3') with increasing irradiation temperature (see Fig. 50). This suggests that the traps responsible for the C_3' peak are considered to be a little deeper than those for the C_3'' peak under the short-circuit condition where X-rays are irradiated. Then, trapped carriers can be released more easily from the traps for the C_3'' peak and the number of the carriers stored in them after X-ray-irradiation decreases more rapidly with increasing irradiation temperature. However, as mentioned above, the traps for the C_3' peak become shallower with increasing bias field, while the depth of the traps for the C_3'' peak remains constant. Therefore, the former may be a little shallower under a high bias field of 360 kV/cm than the latter and the C_3' peak appears at a lower temperature than the C_3'' peak. This is a possible reason why the high temperature C_3'' peak disappears at a lower irradiation temperature than the low temperature C_3' peak as shown in Fig. 50.

6. 5. Conclusions

X-ray induced TSC in various kinds of PVDF specimens have been investigated. There are three split TSC peaks, the C_1, C_2 and C_3 in ascending order of temperature. The C_1 and C_2 peaks are due to dipole orientation in amorphous regions, corresponding to the γ- and β-relaxations, respectively. The C_3 peak is due to carrier traps in the α-crystalline phase and / or on its surface.

The field dependence of the TSC revealed that at least two kinds of carrier traps are responsible to the C_3 peak. The carrier release from one kind of trap is strongly affected possibly through the lowering of the trap depth by the electric field.

7. X-ray Induced TSC and TL in Fluorocarbon Polymers

7. 1. Introduction

Fluorocarbon polymers such as polytetrafluoroethylene (PTFE), Teflon FEP and PFA are of a great practical importance because of their superior thermal and chemical resistance, good insulating properties (low tanδ and high resistivity) and excellent charge-storage capability.[102] Therefore, these materials, especially FEP, have received much attention as insulating materials in the high temperature region and also as flexible film materials for the electret devices.[4,103~105]

The excellent charge-strage capability is caused by deep traps. In this chapter, the natures and the origins of carrier traps in fluorocarbon polymers have been investigated by using the X-ray induced TSC and TL techniques.

7. 2. Experimental

Specimens used were commercial films of PTFE, ETFE (ethylene-tetrafluoro-

ethylene copolymer: Afron), Teflon FEP (tetrafluoroethylene-hexafluoropropylene copolymer: FEP 100 A) and PFA (tetrafluoroethylene-perfluoroalkilvinylether copolymer). Their details are summarized in table 1. The experimental procedures were just the same as before.

7. 3. Experimental Results and Discussion

7. 3. 1. PTFE and ETFE

Figure 51 shows the resultant TSC and TL spectra from PTFE, suggesting the existence of many carrier traps. The TSC peaks correspond well to the TL peaks and also to the relaxation temperatures (α, β and γ).[106] In most cases, the relaxation temperatures cited in Chapter 7 and 8 have been estimated from Wada's dispersion maps around 1 c/s,[106] where L indicates local mode relaxation, P primary dispersion, and C relaxation in crystalline part. All the TSC (TL) peaks except C_4 and C_5 peaks correspond to the release of molecular motions. This suggests that the carrier detrapping is closely related to the release of molecular motions and they lie in the regions where the corresponding molecular motions occur as is the case of PE.

The TSC and TL spectra from ETFE are shown in Fig. 52.

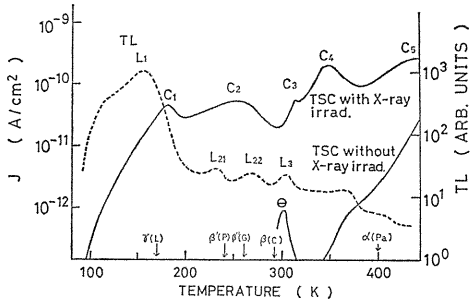

Fig. 51. TSC and TL of PTFE, together with the relaxation temperatures (↓).

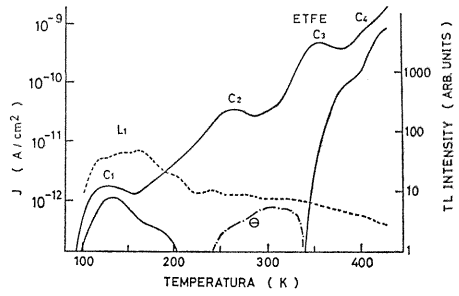

Fig. 52. TSC and TL of ETFE.

7. 3. 2. Teflon FEP and PFA

Figure 53 shows the TSC and TL spectra from FEP, together with the relaxation temperatures. There exist six TSC peaks due to trapped carriers and all TSC (TL) peaks except C_3 and C_4 peaks seem to correspond to the release of molecular motions.

It was reported that there were two crystalline phase transitions at 292 and 303K in PTFE[107,108] and Ranicar and Fleming[109] observed two corresponding TSC peaks in this temperature region. As the crystalline in FEP is considered to be similar to that of PTFE, the couple of two sharp peaks, C_3 and C_4, may be related to such crystalline transitions. The release of carriers in FEP is, therefore, also suggested to be in close relation to molecular motions.

As shown in Fig. 54, the apparent trap depths responsible for these peaks were estimated around 0. 1–1. 2eV applying the initial rise method.

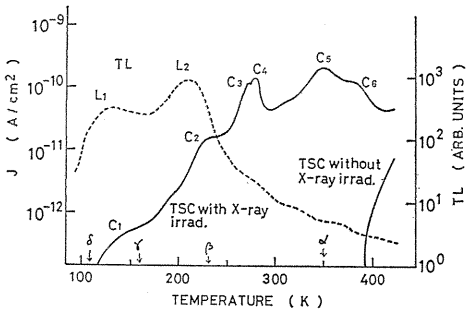

Fig. 53. TSC and TL of Teflon FEP, together with the relaxation temperatures (↓).

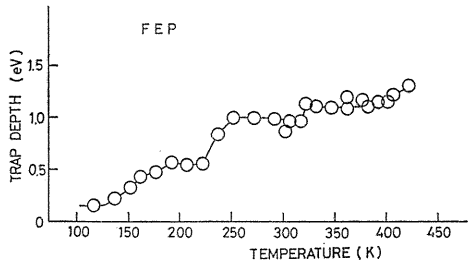

Fig. 54. Apparent trap depth E_t plotted against the maximum temperature reached in each partial heating.

Figures 55 and 56 show the field dependence of TSC with X-ray irradiation. Unlike in high density polyethylene, peak temperatures scarcely change with an applied field. This suggests that the release of carriers in FEP is more strongly dominated by molecular motions. As shown in Fig. 56 peak currents for C_1–C_5 increase almost linearly with a field but the C_6 peak show a somewhat anomalous behaviour.

The C_3 and C_4 peaks having no corresponding relaxations disappeared in the FEP specimen irradiated with 1.8 Mrad of the γ-rays (Fig. 57). Their origins

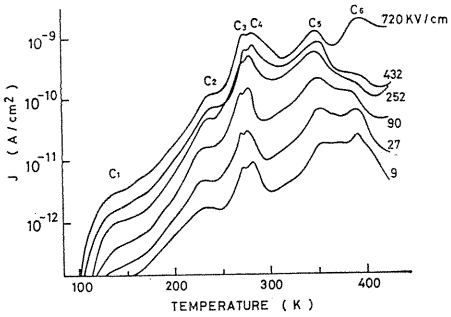

Fig. 55. Field dependence of TSC spectra of FEP.

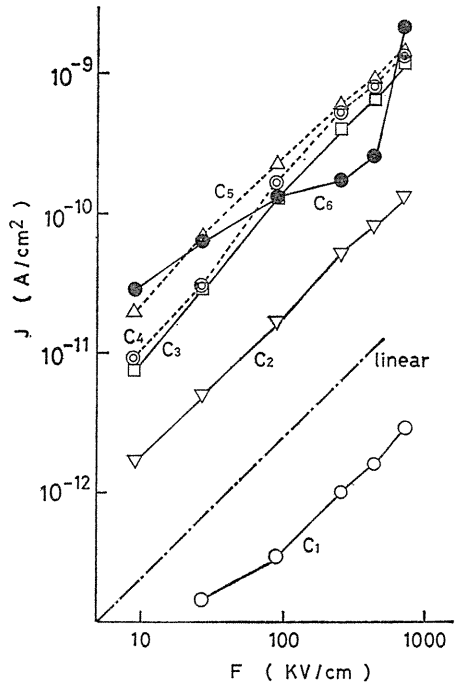

Fig. 56. Field dependence of TSC peak currents.

seem to be unstable defects.

Figure 58 shows the TSC spectra from PFA, which has the structure with the $-O-C_3F_7$ instead of the $-CF_3$ in FEP. The TSC spectrum of Teflon PFA is very similar to that of FEP.

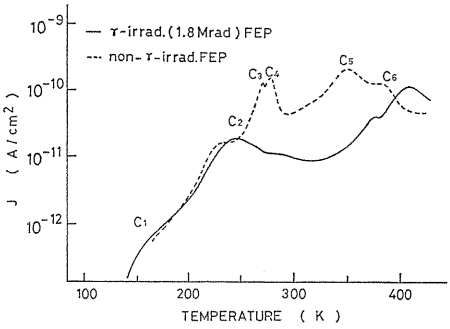

Fig. 57. TSC spectra of γ-irradiated FEP.

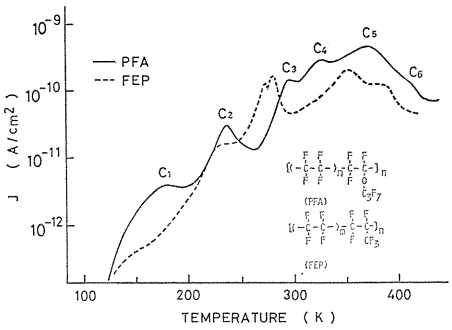

Fig. 58. TSC spectra of Teflon PFA.

7. 4. Conclusions

The TSC and TL spectra from fluorinated polymers (PTFE, ETFE, FEP and PFA) revealed the existence the abundance of carrier traps. Generally, fluorinated polymers show remarkable TSC peaks in the high temperature region compared with polyethylene, which suggests the existence of deep traps. This is the reason for their good charge-storage capabilities.

Most of the TSC and TL peaks are associated with the release of molecular motions, suggesting the close relation between carrier detrapping and molecular motion.

8. X-ray Induced TSC and TL in Other Insulating Polymers

8. 1. Introduction

As seen in the previous chapters, the X-ray induced TSC and TL gave a lot of information about the natures and the origins of carrier traps in PE and fluorocarbon polymers. In this chapter, the X-ray induced TSC and TL spectra of other insulating polymers have been briefly discussed.

8. 2. Experimental

Specimens used here were films of polypropylene (PP), poly-p-xylylene (PPX), polyethylene terephthalate (PET), polycarbonate (PC), polystyrene (PS), polyvinyl chloride (PVC), polyvinyl fluoride (PVF) and nylon 6. They are listed in Table 2. In all cases, specimens were irradiated with X-rays (35 kV, 20 mA) for 20 minutes and the experimental procedures of TSC and TL were just the same as in the previous chapters.

8. 3. *Experimental Results and Discussion*

8. 3. 1. *Polypropylene (PP)*

Figure 59 shows the resultant TSC and TL spectra in PP, together with the relaxation temperatures estimated from Wada's dispersion maps around 1 c/s.[106] The TSC and TL spectra of PP are very similar to those of PE and suggest an abundance of carrier traps. As shown in Fig. 59, the C_2 and L_2 peaks correspond to the γ-relaxation and the C_3 and L_3 peaks to the β-relaxation in amorphous regions. However, the C_4 peak which is considered to correspond to the C_4 peak in PE has no corresponding dispersion. Minami et al. reported the peak of loss tangent around 320 K due to a paracrystalline smetic phase,[110] and Wada and Hotta reported the glass transition in the amorphous region which is rich in the isotactic phase around 290 K.[111] Therefore, it is possible that these transition are responsible for the C_4 peak.

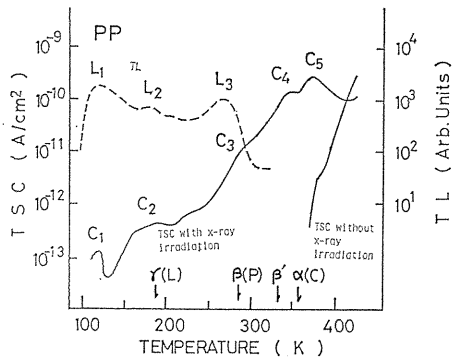

Fig. 59. TSC and TL spectra of PP.

8. 3. 2. *Poly-p-xylylene (PPX)*

Thin PPX films in thickness ranging from 0.002 to several tens μm are easily deposited onto a substrate kept at room temperature by the vapour-phase polymerization.[112] Their various applications will be expected.

Figure 60 shows the resultant TSC and TL in PPX films, together with the relaxation temperatures obtained by the mechanical loss measurement.[113] The PPX shows five TSC peaks originating from trapped carriers and the TSC C_1 and C_2 peaks are accompanied with the TL L_1 and L_2 peaks. Judging from the relaxation temperatures, the C_2 and C_5 peaks seem to correspond to the γ and β relaxations, respectively.

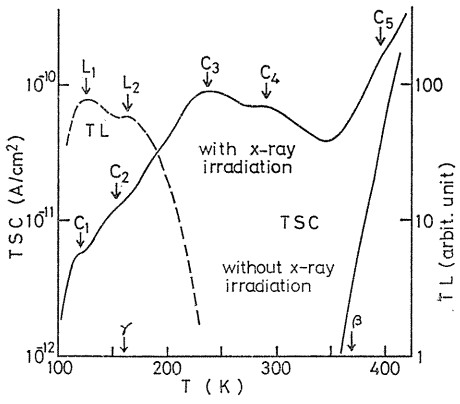

Fig. 60. TSC and TL spectra of PPX.

Here, the $C_1(L_1)$ peak will be discussed. PPX is linear and highly crystalline polymer.[112] Polyethylene, one of the linear and crystalline polymers shows a TSC (TL) peak at 120–130 K which is followed by the TSC (TL) peak at 160–170 K corresponding to the γ relaxation.[12] Nara et al.[76] pointed out the existence of the δ relaxation at 120 K from the free radical decay characteristics of polyethylene, suggesting the correlation between the TSC peak at 120–130 K and the δ relaxation. On the analogy of the result of PE, the C_1 (L_1) peak suggests the existence of a new relaxation in PPX, called the δ

relaxation.

No relaxation corresponding to the C_3 and C_4 peaks, the most remarkable peaks have been observed yet in PPX. Therefore, regardless of molecular motions, carriers are thermally released from traps responsible for the C_3 and C_4 peaks. Their apparent trap depth is 0.5–0.6 eV from the partial heating method.[24]

8. 3. 3. Polyethylene terephthalate (PET), polycarbonate (PC) and polystyrene (PS)

Figures 61–63 show the resultant TSC and TL spectra of PET, PC and PS. These polymers are low-crystalline or amorphous polymers and they show no remarkable TSC (TL) peaks in high temperature region above the glass transition temperature. The TSC (TL) peaks due to trapped carriers correspond well to the relaxation temperatures.

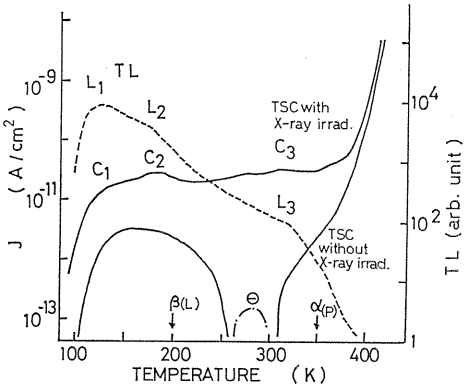

Fig. 61. TSC and TL spectra of PET.

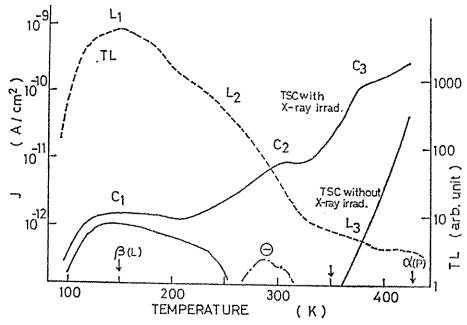

Fig. 62. TSC and TL spectra of PC.

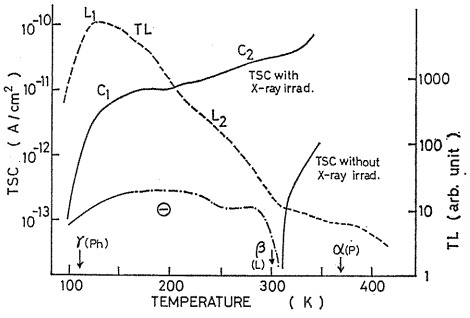

Fig. 63. TSC and TL spectra of PS.

As to PET, Hino[114] reported a broad TSC peak around 170 K due to dipole depolarization associated with local mode relaxation. In this temperature region, Takai et al. reported a TSC peak from PET photoelectrets which corresponds to the molecular motion of the COO group in the main chain.[115] The C_1 (L_1) peak is related to this molecular motion. The shoulder in the TL spectrum around 320 K may be associated with the glass transition, but the corresponding TSC peak is

not clear. The TSC peak without X-ray irradiation around 160 K followed by a current inversion has the characteristics of a peak due to the dipole orientation as discussed in § 2. 3.

As to PC (Fig. 62), the comparative small difference in TSC in the β relaxation region suggests a large contribution of dipoles to the C_1 peak. However, the intensive TL also suggests a considerable amount of electron traps exciting in this region. The C_2 peak is apparently not associated with relaxation. Takamatsu and Fukada also reported TSC peaks from thermoelectrets aroud 280–320 K, which were influenced by streching of PC films.[116] Krum and Müller reported a peak in tan δ around 350 K at 1 kHz in a stretched PC film.[117] Therefore, the C_2 peak is possibly associated with molecular motions in the intermediate phase introduced by stretching.

The large difference between TSC with and without X-ray irradiation as well as the intense TL suggests an abundance of electronic trapping sites in PS (Fig. 63). However, the TSC spectrum is monotonous and no remarkable split peak can be observed. The L_1 peak and the corresponding TSC are considered to be associated with the relaxation of phenyl groups.

8. 3. 4. Polyvinyl chloride (PVC), polyvinyl fluoride (PVF) and nylon 6

In these polymers, the differences between TSC with and without X-ray irradiation are so small that the observed TSC is suggested to originate from ionic[108, 109] and / or dipole orientation. Moreover, their TL was scarcely observed. Typical TSC spectra of PVC and Nylon 6 are shown in Figs. 64 and 65. The X-ray induced TSC and TL techniques are not effective for these polymers.

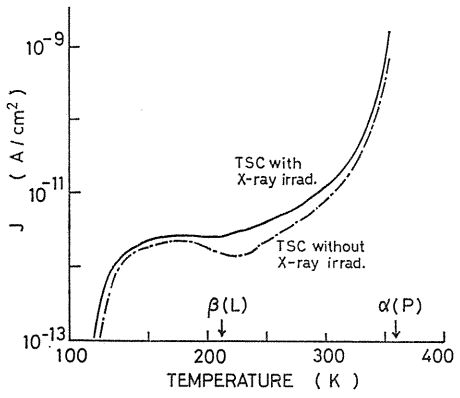

Fig. 64. TSC spectra of PVC.

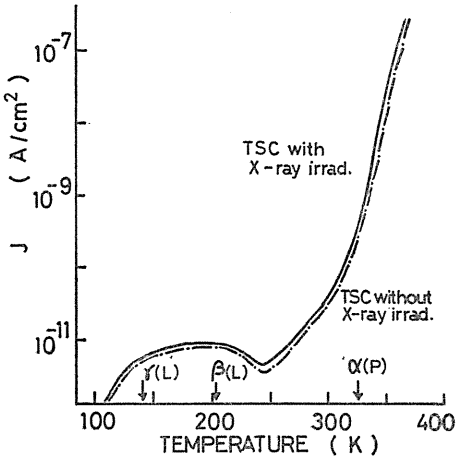

Fig. 65. TSC spectra of Nylon 6.

8. 4. Conclusions

Generally, the TSC (TL) peaks due to trapped carriers in polymers correspond well to the relaxation temperatures. The detrapping of carriers from traps is closely related to the onset of the molecular motions.

Semicrystalline polymers such as PP and PPX show many TSC peaks above

their glass transition temperatures, suggesting the existence of many traps in crystalline parts and / or crystalline surfaces.

The X-ray induced TSC and TL techniques are not effective for polymers which show a large ionic conduction.

9. Summary

The natures and the origins of carrier traps in polymers have not yet been well understood, though they are necessary in order to understand the electrical properties of polymers. In this paper, it has been pointed out that the X-ray induced TSC and TL techniques are very useful to investigate the natures and the origins of carrier traps and these techniques have been systematically applied to various insulating polymers,

The resultant X-ray induced TSC and TL revealed the existence of carrier traps in polymers and gave a lot of information about their natures and origins. Since the detrapping of carriers from traps was frequently enhanced by the release of molecular motions, some of traps were concluded to lie in the regions where the corresponding molecular motions occur. Some carrier traps were considered to originate from microcavities formed by local arrangements of molecular chains. In this case, the detrapping of electrons is closely related to the molecular motions and the TSC (TL) spectrum depends upon the morphology of polymers. In PE, oxidation products such as carbonyl groups and the cross-linking point also acted as deep traps. The details of the conclusions obtained in this paper have been already described at the end of each chapter.

These results about carrier traps in polymers will provide useful clues to solve problems confronting the practical use of polymeric materials for electrical purposes, to lead to improved morphological and chemical design of polymers and also to develop new practical applications.

Acknowledgement

The authors would like to express their gratitude to Mitsubishi Petrochemical Co. Ltd. and Kureha Chemical Industries for the supply of PE and PVDF films. This work was supported in part by the Shinsei Shigen Kyokai and by the Grant-in-Aid for Scientific Research from the Ministry of Education, Science and Culture.

References

1) A. Bradwell, R. Cooper and B. Varlow: Proc. IEE **118** (1971) 247.
2) M. Ieda and M. Nawata: IEEE Trans. **EI-12** (1977) 19.
3) M. Ieda: IEEE Trans. **EI-15** (1980) 206.
4) G. M. Sessler: "Electrets" (Springer-Verlag, Berlin, 1980).
5) F. W. Schmidlin: "Electrophotography" in "Photoconductivity and Related Phenomena" ed. by J. Mort and D. M. Pai (Elsevier, Amsterdam, 1976) p. 42.
6) G. M. Sessler and J. E. West: Chap. 7 in "Electrets" ed. by G. M. Sessler (Springer-

Verlag, Berlin, 1980) p. 347.
7) J. van Turnhout: "Thermally Stimulated Discharge of Polymer Electrets" (Elsevier, Amsterdam, 1975).
8) M. Dole: "The Radiation Chemistry of Macromolecules (Academic Press, New York, 1972) vol. **1**, pp. 193-222.
9) P. Braunlich: "Thermally Stimulated Relaxation in Solids" (Springer Verlag, Berlin, 1979).
10) M. Ieda, Y. Suzuoki and T. Mizutani: Kobunshi Ronbunshu **36** (1979) 671.
11) S. W. S. McKeever and D. M. Huges: J. Phys. D Appl. Phys. 8 (1975) 1520.
12) T. Mizutani, Y. Suzuoki and M. Ieda: J. Appl. Phys. **48** (1977) 2408.
13) T. Mizutani, Y. Suzuoki and M. Ieda: Trans. IEE Japan **96-A** (1976) 419. R. R. Haering and E. N. Adams: Phys. Rev. **117** (1960) 451.
14) G. F. J. Garlick and A. F. Gibson: Proc. Phys. Soc. (London) **60** (1948) 574.
15) P. Berticat, A. Bui, H. T. Giam, D. C. Chatain and C. Lacabanne: Macromol. Chem. **177** (1976) 1583.
16) P. Fischer and P. Rohl: J. Poly. Sci. Polym. Phys. Ed. **14** (1976) 531.
17) T. Mizutani and M. Ieda: J. Phys. D Appl. Phys **11** (1978) 185.
18) A. E. Blake, A. Charlesby and K. J. Randle: J. Phys. D Appl. Phys. **7** (1974) 759.
19) I. Boustead and A. Charlesby: Proc. Roy. Soc. **A316** (1970) 291.
20) K. Amakawa and Y. Inuishi: Trans IEE Japan **93-A** (1973) 533.
21) T. Nishitani, K. Yoshino and Y. Inuishi: Jpn. J. Appl. Phys. **14** (1975) 721.
22) V. G. Nikolskii, V. A. Tochin and N. Ya. Buben: Soviet Physics-Solid State **5** (1964) 1636.
23) M. M. Eidel'nant, F. I. Duntov, V. Kh. Krundel and B. I. Sazhin: Polym. Sci. USSR **A15** (1973) 601.
24) R. A. Creswell and M. M. Perlman: J. Appl. Phys. **41** (1970)2365.
25) J. F. Fowler: Proc. Roy. Soc. (London) **A236** (1965) 464.
26) J. M. Andre, G. S. Kapsomenos and G. Leroy: Chem. Phys. Lett. 8 (1971) 195.
27) J. Delhalle. J. M. Andre, S. Delhalle, J. J. Pireaux, R. Candano and J. J. Verbist: J. Chem. Phys. **60** (1974) 595.
28) L. E. Nielsen: J. Polym. Sci. **42** (1960) 357.
29) Ref. 6, p. 83.
30) H. A. Flocke: Kolloid-Z. **180** (1962) 118.
31) A. Ekstrom and J. E. Willard: J. Phys. Chem. **72** (1968) 4599.
32) A. Charlesby and R. H. Partridge: Proc. Roy. Soc. (London) **A271** (1963) 170.
33) V. G. Nikolskii, L. Yu. Zlatkevich, M. B. Konstaninopolskaya, L. A. Osintseva and V. A. Sokolskii: J. Polym. Sci. Polym. Phys. Ed. **12** (1974) 1267.
34) M. Ieda, M. Kosaki, Y. Yamada and U. Shinohara: 1964 Ann. Rept. Conf. on Electrical Insulation (NAS-NRC, Washington, 1964) p. 29.
35) D. K. Davis: J. Phys. D Appl. Phys. **5** (1962) 162.
36) J. Frenkel: Phys. Rev. **54**(1967) 647.
37) Y. Suzuoki, K. Yasuda, T. Mizutani and M. Ieda: Jpn. J. Appl. Phys. **17** (1978) 1215.
38) C. G. Garton and N. Parkman: Proc. IEE. **123** (1976) 271.
39) N. F. Mott and R. W. Gurney: "Electronic Processes in Ionic Crystals" (Clarender Press, Oxford, 1940) p. 86.
40) Y. Suzuoki, T. Mizutani, Y. Takai and M. Ieda: Jpn. J. Appl. Phys. **16** (1977) 1929.
41) Y. Takai, K. Mori, T. Mizutani and M. Ieda: Jpn. J. Appl. Phys. **15** (1976) 2441.
42) Y. Takai, K. Mori, T. Mizutani and M. Ieda: Jpn. J. Appl. Phys. **16** (1977) 1937.
43) J. D. Brodribb, D. O. Colmain and D. M. Hughes: J. Phys. D: Appl. Phys. 8 (1975) 856.
44) M. M. Perlman and S. Unger: J. Phys. D: Appl. Physs. **5** (1972) 2115.
45) Y. Suzuoki, K. Yasuda, T. Mizutani and M. Ieda: J. Phys. D: Appl. Phys. **10** (1977) 1985.
46) B. Ranby and J. F. Rabek: "Photodegradation, Photo-oxidation and Photostabilization of Polymers" (Bristol, Wiley, 1975) p. 353.
47) R. W. Murraay: Acc. Chem. Res. **1** (1968) 313.

48) G. D. Cooper and M. Prober: J. Polym. Sci. **44** (1960) 397.
49) A. D. Delman, B. B. Simms and A. E. Ruff: J. Polym. Sci. **45** (1960) 415.
50) T. Mizutani and M. Ieda: J. Phys. D: Appl. Phys. **12** (1979) 291.
51) T. Mizutani, T. Tsukahara and M. Ieda: J. Phys. D: Appl. Phys. **13** (1980)
52) A. Many and G. Rakavy: Phys. Rev. **126** (1962) 1980.
53) T. Mizutani, T. Tsukahara and M. Ieda: Jpn. J. Appl. Phys. **19** (1980)
54) S. Nakamura, G. Sawa, T. Mizutani and M. Ieda: Trans. IEE Japan **94-A** (1974) 477.
55) S. Nakamura, G. Sawa, T. Mizutani and M. Ieda: Trans. IEE Japan **95-A** (1975) 255.
56) M. L. McCubbin and I. D. C. Gurney: J. Chem. Phys. **43** (1965) 483.
57) W. L, McCubbin: J. Polym. Sci. **C-30** (1970) 181.
58) W. L. McCubbin and R. Mamo: Chem. Phys. Lett. **2** (1968) 230.
59) K. Morokuma: J. Chem. Phys. **54** (1971) 1962.
60) J. Andre: Chem. Phys. Lett. **14** (1972) 485.
61) D. L. Beveridge, I. Jano and L. Ladik: J. Chem. Phys. **56** (1972) 4744.
62) J. Andre and G. Leroy: Chem. Phys. Lett. **5** (1971) 71.
63) A. Imamura: J. Chem. Phys. **52** (1970) 3168.
64) M. H. Wood, M. Borber I. H. Hillier and J. M. Thomas: J. Chem. Phys. **56** (1972) 1788.
65) C. Baird and M. J. S. Dewar: J. Chem. Phys. **50** (1969) 1262.
66) M. J. S. Dewar, S. H. Suck and P. K. Weiner: Chem. Phys. Lett. **15** (1974) 220.
67) O. Kikuchi: A series of monographs modern trends in chemistry Vol. **6** "Bunshi Kidoho" (Kodansha, Tokyo, 1971).
68) B. L. Beveridge and W. Wun: Chem. Phys. Lett. **17** (1972) 554.
69) M. Fujishima and H. Inokuchi: J. Chem. Phys. **56** (1972) 1788.
70) R. A. George, D. M. Martin and E. G. Wilson: J. Phys. C **5** (1972) 871.
71) K. J. Less and E. G. Wilson: J. Phys. C **6** (1973) 310.
72) K. Seki, S. Hashimoto, N. Sato, Y. Harada, K. Ishii and J. Kanbe: J. Chem. Phys. **66** (1977) 3644.
73) A. Charlesby and R. H. Partridge: Proc. Roy. Soc. **A283** (1965) 312.
74) I. Boustead and A. Charlesby: European Polym. J. **3** (1967) 459.
75) J. H. Ranicar and R. J. Fleming: J. Polym Sci. Polym. Phys. Ed. **10** (1972) 1979.
76) S. Nara, S. Shimada, H. Kashiwabara and J. Sohma: J. Polym. Sci. **A-2**, 6 (1968) 1435.
77) M. Kakizaki and T. Hideshima: Repts. Prog. Polym. Phys. Japan. **11** (1968) 351.
78) S. Nakamura, M. Ieda and G. Sawa: J. Appl. Phys. **48** (1977) 179.
79) A. C. Somersall, E. Dan and J. E. Guillet: Macromolecules **7** (1974) 233.
80) M. G. Broadhurst and G. T. Davis: "Piczo and Pyroelectric Properties" in "Electrets" ed. by G. M. Sessler (Springer-Verlag, Berlin, 1980) p. 285.
81) R. D. Parker: NASA Report CR124926 (1976)
82) W. M. Prest and D. J. Luca: J. Appl. Phys. **49** (1978) 5042.
83) D. K. Das Gupta and K. Doughty: J. Appy. Phys. **49** (1978) 4601.
84) D. K. Davis, J. E. McKinney, M. G. Broadhurst and S. C. Roth: J. Appl. Phys. **49** (1978) 4998.
85) J. B. Lando, H. L. Olf and A. Peterlin: J. Polym. Sci. A-1, **4** (1966) 941.
86) G. Pfister, M. Abkowitz and R. G. Crystal: J. Appl. Phys. **44** (1973) 3360.
87) N Murayama, T. Oikawa, T. Kato and K. Nakamura: J. Polym. Sci.: Polym. Phys. Ed. **13** (1975) 1033.
88) N. Murayama: J. Polym. Sci.: Polym. Phys. Ed. **16** (1978) 929.
89) H. Sussner and K. Dransfeld: J. Polym. Sci.: Polym. Phys. Ed. **16** (1978) 529.
90) T. Takamatsu and E. Fukada: Polym. J. **1** (1970) 101.
91) G. Pfister, W. M. Prest, D. J. Luca and M. Abkowitz: Appl. Phys. Lett. **27** (1975) 486.
92) G. Pfister and M. Abkowitz: J. Appl. Phys. **46** (1974) 1001.
93) M. Abkowitz and G. Pfister: J. Appl. Phys. **46** (1975) 2559.
94) N. Murayama and H. Hashizume: J. Polym. Sci.: Polym. Phys. Ed. **14** (1976) 989.
95) T. Mizutani, N. Sugiura, Y. Suzuoki and M. Ieda: Jpn. J. Appl. Phys. **20** (1981) 59.
96) S. Yano, K. Tadano, K. Aoki and N. Koizumi: J. Polym. Sci.: Polym. Phys. Ed. **12**

(1974) 1875.
97) Y. Suzuoki, T. Mizutani, M. Shimozato, N. Sugiura and M. Ieda: Jpn. J. Appl. Phys. **19** (1980)861.
98) S. Yano: J. Polym. Sci. A-2 8 (1970) 1057.
99) H. Kakutani: J. Polym. Sci. A-2, ,8 (1970) 1177.
100) H. Sasabe, S. Saito, M. Asahina and H. Kakutani: J. Polym. Sci. A-3, **7** (1969) 1405.
101) R. F. Boyer: J. Polym. Sci.: Polym. Symp. **50** (1975) 189.
102) R. A. Creswell, M. M. Perlman and K. Kabayama: "Dielectric Properties of Polymers" ed. by E. E. Karasz (Plenum Press, New York, (1972) p. 295.
103) G. M. Sessler and J. E. West: Phys. Rev. **B-10** (1974) 4488.
104) B. Gross, G. M. Sessler and J. E. West: J. Appl. Phys. **45** (1974) 2841. Appl. Phys. Lett. **24** (1974) 351, J. Appl. Phys. **47** (1976) 968.
105) K. Ikezaki, K. Wada and I. Fujita: J. Electrochem. Soc. **122** (1975) 1356.
106) Y. Wada: "Kobunshi no Kotai Bussei" (Baifukan, Tokyo. 1971) p. 391.
107) A. Mele, A. D. Site, C. Bettinali and A. Didomenico: J. Chem. Phys. **49** (1968) 3297.
108) G. T. Furukawa, R. E. McCoskey and G. J. King: J. Res. Nat. Bur. Stand. **49** (1952) 273.
109) J. H. Ranicar and R. J. Fleming: J. Polym. Sci.: Polym. Phys. Ed. **10** (1972) 1979.
110) S. Minami, S. Uemura and M. Takayanagi: Repts. Prog. Polym. Phys. Japan. **7** (1964) 253.
111) Y. Wada and Y. Hotta: J. Polym. Sci. C-**23** (1968) 583.
112) W. F. Gorham: J. Polym. Sci. A-1, **4** (1966) 3027.
113) C. H. Chung and J. A. Sauer: J. Polym. Sci. A-2, **9** (1971) 1097.
114) T. Hino: Trans. IEE Jpn. **93-A** (1973) 449.
115) Y. Takai, K. Mori, T. Mizutani and M. Ieda: Jpn. J. Appl. Phys. **16** (1977) 1937.
116) T. Takamatsu and E. Fukada: Rept. of IPCR **46** (1970) 47.
117) F. Krum and Muller: Kolloid Z **164** (1959) 81.
118) D. A. Seanor: J. Polym. Sci. **A-2** (1968) 463.
119) M. Kosaki, H. Ohshima and M. Ieda: J. Phys. Soc. Jpn. **29** (1970) 1012.